

USE OF REMOTE SENSING FOR FRACTURE DISCRIMINATION  
AND ASSESSMENT OF POLLUTION SUSCEPTIBILITY OF  
A LIMESTONE-CHERT AQUIFER IN  
NORTHEASTERN OKLAHOMA

By

ESMAEIL AZIMI

Bachelor of Science

Azarabadegan University

Tabriz, Iran

1975

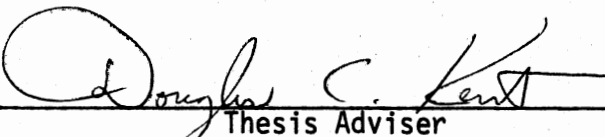
Submitted to the Faculty of the Graduate College  
of the Oklahoma State University  
in partial fulfillment of the requirements  
for the Degree of  
MASTER OF SCIENCE  
December, 1978

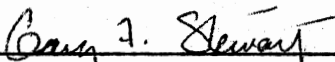
Thesis  
1978  
A995u  
cop. 2

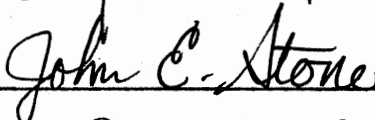


USE OF REMOTE SENSING FOR FRACTURE DISCRIMINATION  
AND ASSESSMENT OF POLLUTION SUSCEPTIBILITY OF  
A LIMESTONE-CHERT AQUIFER IN  
NORTHEASTERN OKLAHOMA

Thesis Approved:

  
\_\_\_\_\_  
Thesis Adviser

  
\_\_\_\_\_

  
\_\_\_\_\_

  
\_\_\_\_\_  
Dean of the Graduate College

1019362

## PREFACE

This study is concerned with using analogous and digitally-enhanced remotely sensed data for discrimination of fracturing (and of related pollution susceptibility and recharge) in an unconfined limestone-chert aquifer in the Ozark region of northeastern Oklahoma. Skylab-4 photography was used for regional structural mapping. LANDSAT photographs, Skylab, and digitally-enhanced data were used for the detailed study of the area.

The author wishes to express a sincere debt of gratitude to his major adviser, Dr. Douglas C. Kent, for his suggestion of the problem, guidance, assistance, friendly attitude toward international students, and encouragement throughout his graduate studies. Appreciation is also expressed to Dr. John E. Stone and Dr. Gary F. Stewart, committee members, for their invaluable guidance, comments, and suggestions on the final manuscript. Gratitude is also expressed to Dr. William D. Warde, statistician, Statistics Department, for his assistance and valuable comments on the statistics used in this study.

Appreciation is also extended to Mr. Glen Hair and Mr. Bill Smith, Department of Environmental Health in Tahlequah and Claremore, Oklahoma, respectively, for providing the water quality data.

The author also expresses his deep affection and gratitude to his father for his encouragement, unfailing support, and wise criticism

during these studies.

Finally, special gratitude is expressed to my wife for her understanding, encouragement, and continuous support during my graduate studies.

## TABLE OF CONTENTS

Chapter	Page
I. INTRODUCTION . . . . .	1
Objectives . . . . .	2
Methodology . . . . .	3
Regional Study . . . . .	3
Detailed Study of Linears . . . . .	4
II. THE STUDY AREA . . . . .	7
Location . . . . .	7
Climate . . . . .	7
Soil . . . . .	8
Alluvial Soils . . . . .	8
Fragipan Soils . . . . .	14
Limestone Residuum Soils . . . . .	14
Land Use . . . . .	14
III. GEOLOGY AND HYDROGEOLOGY . . . . .	17
Physiographic Setting . . . . .	17
Stratigraphy . . . . .	19
Regional Structure . . . . .	19
Ground Water . . . . .	22
Source and Movement . . . . .	22
Ground-water Quality . . . . .	24
IV. ANALYSIS OF LINEARS FOR POLLUTION SUSCEPTIBILITY AND WATER QUALITY . . . . .	28
Previous Investigations . . . . .	29
Local and Adjacent Areas . . . . .	29
Other Areas . . . . .	31
Data Processing . . . . .	32
Standard LANDSAT Imagery . . . . .	32
Computer-enhanced Digital Data . . . . .	32
Skylab-4 190A Photographs . . . . .	34
Linear Evaluation Methods . . . . .	35
Linear Evaluation - Results . . . . .	48
Pollution Susceptibility . . . . .	49
Statistical Analyses of Water Quality for Pollution Susceptibility Evaluation . . . . .	58
Method . . . . .	58
Results . . . . .	64

Chapter	Page
V. SUMMARY OF RESULTS . . . . .	73
Linears . . . . .	73
Pollution Susceptibility . . . . .	74
Recommendations for Future Studies . . . . .	75
BIBLIOGRAPHY . . . . .	76
APPENDIX A - GEOLOGIC FORMATION CHARACTERISTICS . . . . .	79
APPENDIX B - WATER QUALITY SAMPLE LOCATIONS . . . . .	87
APPENDIX C - VARIANCE TABLES FOR F-DISTRIBUTION . . . . .	90
APPENDIX D - PROCEDURE OF ANALYSES OF WATER QUALITY DATA FOR F-TEST DISTRIBUTIONS . . . . .	95

## LIST OF TABLES

Table	Page
I. Range of Temperature in the Subscene Study Area . . .	9
II. Precipitation in the Subscene Study Area . . . . .	10
III. Summary of Chemical Analyses of Water Samples . . . .	26
IV. Summary of Chemical Analyses of Water Samples Collected by the Author . . . . .	27
V. Comparison of Linear Densities . . . . .	48
VI. Comparison of Number of Intersections . . . . .	49
VII. Criteria for Identification of Pollution Suscepti- bility Classes . . . . .	51
VIII. Comparison of Pollution Susceptibility Maps . . . . .	57
IX. Chemical Analyses of Water Collected by the Author From Wells and Springs . . . . .	60
X. Chemical Analyses of Water Samples . . . . .	61
XI. Statistical Analyses of Water Quality for Pollution Susceptibility Classes Derived From Standard LANDSAT Imagery . . . . .	63
XII. Statistical Analyses of Water Quality for Pollution Susceptibility Classes Derived From Digital Imagery	65
XIII. Statistical Analyses of Water Quality for Pollution Susceptibility Classes Derived From Skylab Photography	66
XIV. Statistical Analyses of Water Quality for Pollution Susceptibility Classes Derived From Digital Composite Imagery . . . . .	67
XV. Statistical Analyses of Water Quality for Pollution Susceptibility Classes Derived From Drainage Map . .	68
XVI. Statistical Analyses of Water Quality for Pollution Susceptibility Derived from Skylab Photography . . .	69



Table	Page
XVII. Summary of F-Test Significance Between Pollution Susceptibility Classes . . . . .	70
XVIII. Summary of Statistical Means for Chemical Constituents . . . . .	71
XIX. Water Quality Sample Locations . . . . .	88
XX. Analyses of Variance Table for Chemical Constituents Related to Pollution Susceptibility Classes Derived From Standard LANDSAT Imagery . . . . .	91
XXI. Analyses of Variance Table for Chemical Constituents Related to Pollution Susceptibility Classes Derived From Digital Imagery . . . . .	92
XXII. Analyses of Variance Table for Chemical Constituents Related to Pollution Susceptibility Classes Derived From Skylab Photography . . . . .	93
XXIII. Analyses of Variance Table for Chemical Constituents Related to Pollution Susceptibility Classes Derived From Composite Digital Imagery . . . . .	94

## LIST OF FIGURES

Figure	Page
1. Location Map of Regional and Subscene Study Area . . . . .	5
2. Ranges of Average Temperature of Subscene Study Area for the Month LANDSAT Imagery and Skylab Photography Were Taken . . . . .	11
3. Hydrograph of Daily Precipitation Evaporation, and Discharge of Subscene Study Area for the Month LANDSAT Imagery and Skylab Photographs Were Taken . . . . .	12
4. Soil Map of the Subscene Study Area . . . . .	13
5. Land Use Map of the Subscene Study Area . . . . .	16
6. Physiographic Provinces of the Ozark Uplift and Adjoining Areas . . . . .	18
7. Stratigraphic Column for the Regional and Subscene Areas	20
8. Generalized Geologic and Structural Map of the Subscene Study Area . . . . .	21
9. Generalized Structural Map of the Regional Study Area, Northeastern Oklahoma . . . . .	23
10. Graphs of Mean Daily Stream Discharge, Daily Precipi- tation, Monthly Springflow, and 5-day Ground-water Level for the Subscene Study Area . . . . .	25
11. Orientation Histograms of LANDSAT Linears, Drainage and Joints in the Subscene Area . . . . .	30
12. Data Processing Chart . . . . .	33
13. Linear Map of the Subscene Study Area Derived From Standard LANDSAT Imagery . . . . .	37
14. Linear Map of the Subscene Study Area Derived From Computer-enhanced Digital Imagery . . . . .	38
15. Linear Map of the Subscene Study Area Derived From Skylab-4 S190A Photography . . . . .	39

Figure	Page
16. Linear Density Map of the Subscene Study Area Derived From Standard LANDSAT Imagery (Fig. 13) . . . . .	40
17. Linear Density Map of the Subscene Study Area Derived From Digital LANDSAT Imagery (Fig. 14) . . . . .	41
18. Linear Density Map of the Subscene Study Area Derived From Skylab-4 Photography (Fig. 15) . . . . .	42
19. Drainage Density Map of the Subscene Study Area . . . . .	43
20. Comparison of LANDSAT Linears With Drainage . . . . .	44
21. Number of Intersections Map of the Subscene Study Area Derived From Standard LANDSAT Imagery Linears (Fig. 13)	45
22. Number of Intersections Map of the Subscene Study Area Derived From Computer-enhanced Digital Imagery Linears (Fig. 14) . . . . .	46
23. Number of Intersections Map of the Subscene Study Area Derived From Skylab-4 Linears (Fig. 15) . . . . .	47
24. Pollution Susceptibility Map of the Subscene Study Area Derived From Standard LANDSAT Photography . . . . .	52
25. Pollution Susceptibility Map of the Subscene Study Area Derived From Computer-enhanced Digital Imagery . . . . .	53
26. Pollution Susceptibility Map of the Subscene Study Area Derived From Skylab-4 Photography . . . . .	54
27. Pollution Susceptibility Map of the Subscene Study Area Derived From Composite Digital Imagery . . . . .	55
28. Pollution Susceptibility Map of the Subscene Study Area Derived From Drainage Data . . . . .	56
29. Location Map of Springs and Wells . . . . .	59

## CHAPTER I

### INTRODUCTION

The increased demand of our society for a high quality water supply and concern for our water resources is an important problem. This increased demand requires basic data on the availability and usability of water in many parts of the state and to provide planners and individual rural and urban water users with sufficient data for the development and wise use of this important resource.

Geologic structures such as fractures and joints affect the occurrence and pollution of ground water, particularly in areas where water is obtained from springs and wells of high yield or from rocks broken by faulting. The Boone Formation of northeastern Oklahoma, which is the aquifer evaluated in this thesis, is highly fractured and susceptible to pollution; therefore, evaluation of the fracturing is necessary to plan for the protection of the quality of this water.

The quality of ground water is associated with rock and soil type. Water yields from alluvium in the study area is of the best quality, and ground water in contact with shale is of the poorest quality. Ground water occurring in fractured terrain is generally of higher quality unless it is affected by septic effluent. As a result of the rapid increase in population and development in Adair and Delaware Counties, pollution of the ground water in the area within the Boone Formation can be anticipated; this is the major aquifer in the study area.

Therefore, quality of ground water occurring within the fractured media can either be of high quality due to the effects of dilution within the fractures or can be highly polluted due to pollution from surface sources transmitted through the same fractures. Evaluation of fracture distribution is essential in determining areas where residential and industrial development can be permitted without adversely affecting the ground and surface water quality.

### Objectives

Satellite multispectral imagery (LANDSAT and Skylab) have been successfully used for fracture discrimination; therefore, it is conceivable that this technology can lend itself as an inexpensive method for assessing pollution susceptibility by planners who are establishing zones for land use.

This investigation describes the use of standard LANDSAT, Skylab-4 S190A and digitally-enhanced imageries for the discrimination of linears and evaluates relates related pollution susceptibility and recharge in an unconfined chert-limestone aquifer, the Boone Formation in northeastern Oklahoma.

Specific objectives of this investigation include (1) the preparation of pollution susceptibility maps of the area which were prepared by combining linear density maps with the available soil information; (2) comparison of resultant maps, and (3) statistical analysis of ground-water quality.

LANDSAT multispectral scanners (MSS) are the most economical and simplest way to pursue this type of investigation; previous exploration techniques required many man hours. Extended field time for travel,

equipment setup, and data collection increase both the cost and the length of time of the survey period. The cost and on-site survey time can be reduced by decreasing the number of man hours so that a reduction in the amount of time for labor required can be accomplished by the use of remote sensing satellites equipped with multispectral scanners. Advantages of using LANDSAT imagery was attributed by Watts (1977) to (1) availability for all of the earth's surface; (2) availability under different conditions (except cloud cover), and (3) coverage of large areas to be investigated without using tedious and expensive construction of mosaics with aerial photography.

## Methodology

### Regional Study

The LANDSAT (ERTS) scene E-1506-16263 for December 11, 1973, and Skylab-4 S1904 for January 31, 1974, were used for the regional study area that contains all of Adair, Cherokee, Delaware, Sequoyah, Mayes, Muskogee, and Wagoner Counties in northeastern Oklahoma, as well as the western part of Washington and Benton Counties in Arkansas. The regional study of major fractures, especially faults, included an area of 3600 square miles (9324 square kilometers).

The Earth Resource experimental package Skylab-4 S1904 paper print 25.6 inches in size and at a scale of 1:250,000 was used in this investigation. Linears discernible on the imagery were drawn on tracing paper by directly superimposing the tracing paper on the imagery. The resulting linear map was then overlaid onto a geologic map of the same scale.

### Detailed Study of Linears

The detailed study area covers an area of 215 square miles (550 square kilometers) in northern Adair, the southern part of Delaware, and a small portion of Cherokee Counties in northeastern Oklahoma (Fig. 1).

Negative band seven and color slides of Standard LANDSAT photos were projected with a 135 mm slide projector to a scale of 1:24,000. Linears were drawn onto drafting paper for both negative and positive band seven and the false color composite (FCC). A composite linear map of positive and negative band seven and of the color composite were prepared. This composite linear map then was used to prepare maps showing linear density and the number of intersections. In addition, black and white 135 mm slides of Skylab-4 S190A were projected with a 135 mm slide projector to a scale of 1:24,000. Maps were prepared to show linear density and the number of intersections which could be visually discriminated on the Skylab imagery.

Finally, computer-enhanced images derived from LANDSAT imagery were used for discriminating linears. A computer compatible tape (CCT) of Scene E-1506-16263 was used. Image products included the principal components (PC-1 and PC-2) ratio of bands 5/7, and raw bands four, five, six and seven (negative and positive). These products are described in Chapter IV.

The color slides of computer-enhanced images were projected with a 135 mm slide projector to a scale of 1:24,000. Linears from these images were drawn on tracing paper. A composite linear map as well as maps showing linear density and number of intersections maps were

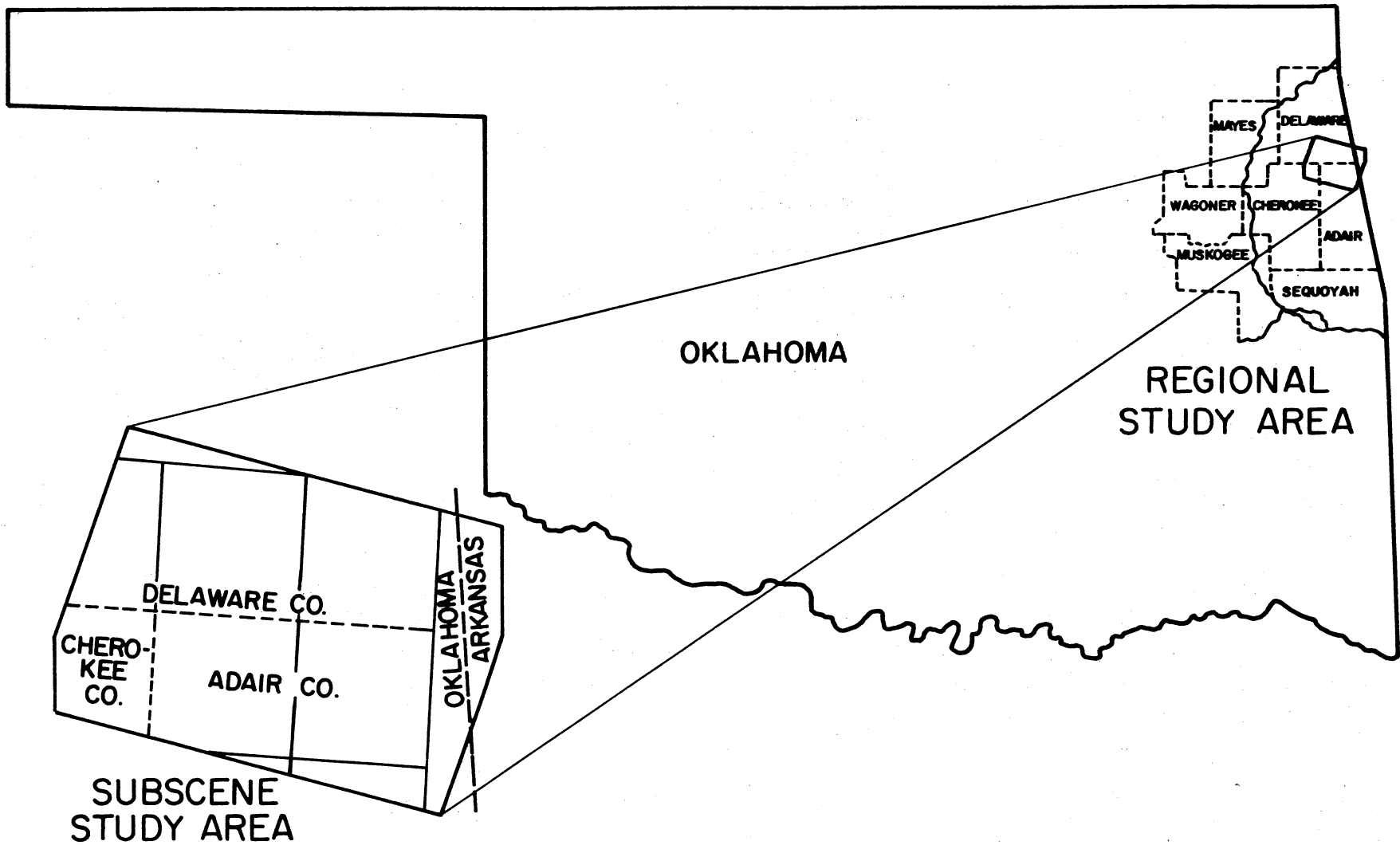


Figure 1 - Location Map of Regional and Subscene Study Area



prepared at the scale of 1:24,000 and reduced to 1:250,000. The linear density map of computer-enhanced images was compared with the linear density map of the standard LANDSAT photographs and Skylab-4.

Drainage maps of the area were prepared from both Army topographic maps and an aerial photography index map. The drainage maps were used to prepare drainage density and pollution susceptibility maps. These maps were compared with the linear, linear density, and pollution susceptibility maps derived from LANDSAT and Skylab products. Water quality data were obtained from open file information and by sample collection in the field. Samples were analyzed for sulfate ( $\text{SO}_4$ ), chloride (Cl), iron (Fe), and total hardness. The statistical analyses of water quality chemical constituents included analysis of variance between ionic species and pollution susceptibility distribution based on linear densities derived from the various LANDSAT and Skylab image products.

## CHAPTER II

### THE STUDY AREA

#### Location

The subscene study area is located entirely within northern Adair, southern Delaware, and northeastern Cherokee Counties in northeastern Oklahoma. The subscene study area is 215 square miles (550 square kilometers) and extends to the eastern boundary of Arkansas. The area is deeply dissected by tributaries to the Illinois River. Watts, Flint Ridge, and the town of Kansas are the largest municipalities in Adair and Delaware Counties. The area is accessible by hard surface and gravel roads. State Highway 33 crosses southeastern Delaware County and State Highways 33 and 59 extend east-west across the area. State Highways 10 and 33C extend southward from State Highways 33 and 59 in Cherokee and Adair Counties.

#### Climate

Delaware, Adair, and Cherokee Counties in northeastern Oklahoma are characterized by a mild seasonal climate with an average annual precipitation of 42 inches and a mean annual temperature of 60<sup>0</sup>F (15.6<sup>0</sup>C). The temperature ranges between -27<sup>0</sup>F (-33<sup>0</sup>C) in winter to 118<sup>0</sup>F (48<sup>0</sup>C) during the summer. The spring, fall, and summer seasons are fair and warm. The range of temperature and precipitation is

shown in Tables I and II, and the hydrograph of average precipitation and temperature range are shown in Figures 2 and 3.

## Soil

Soil characteristics are important in determining pollution susceptibility of ground water because the percolation rate of the soil controls the amount of water which can reach the underlying fractured bedrock. The study area soils consist of three major soil groups: alluvial soils, fragipan soils, and soils developed from limestone. The distribution of these soil groups is shown in Figure 4. Each group consists of several soils series. Soils were classified based on the predominant soil series which occurs within each quarter section using the soil maps provided in the Soil Conservation Service Soil Survey Reports (U. S. Soil Conservation Service, Adair County, 1965, and Delaware and Cherokee Counties, 1970).

### Alluvial Soils

Alluvial soils occur on flood plains and terraces along the major streams and rivers in the area. In the flood plains and benches, the soils are nearly level to gently sloping soils; they are generally deep and are loamy or gravelly. Alluvial soils in Adair County consist of the Etowah, Huntington, Lawrence, and Taft series. Sallisaw, Elash, Staser, Strigle, Taloka, and Verdigris soils are typical of Delaware and Cherokee Counties. Alluvial soils constitute approximately 24 percent of the subscent study area.

TABLE I  
 RANGE OF TEMPERATURE IN THE SUBSCENE STUDY AREA  
 (U.S. Soil Conservation Service, 1970)

Month	Average Daily Maximum (°F)	Average Daily Minimum (°F)	Two years in ten will have at least four days with	
			Maximum Temperature Equal to or Higher than (°F)	Minimum Temperature Equal to or Higher than (°F)
January	49.9	26.7	68	9
February	54.3	29.9	70.5	15
March	61.6	36.6	77.5	19
April	72.3	47.2	84	32
May	79.2	55.4	88	42
June	87.3	63.2	98.5	52.5
July	93.1	67.4	102	60
August	93.3	66.9	104.5	56
September	86.8	58.9	98.5	44
October	75.8	47.8	89.5	33
November	61.3	35.4	76.5	19
December	52.9	29.5	69	16
Year	72.2	47	104 <sup>1</sup>	32 <sup>2</sup>

<sup>1</sup>Average annual maximum.

<sup>2</sup>Average annual minimum.

TABLE II  
 PRECIPITATION IN THE SUBSCENE STUDY AREA  
 (U.S. Soil Conservation Service, 1970)

Month	Average Total (inches)	One Year in ten will have		Days with Snow Cover one inch or more	Average Days with Snow Cover (inches)
		Less than (inches)	More than (inches)		
January	2.14	.4	4.3	3	3
February	2.8	.7	6.2	2	2
March	3.33	.9	7.7	2	3
April	4.72	2.25	9.9	1	2
May	5.99	2.25	12.2	0	—
June	4.94	.7	9.4	0	—
July	3.09	.25	7.7	0	—
August	3.00	.35	5.6	0	—
September	3.93	.5	7.8	0	—
October	3.48	.75	7.9	0	—
November	2.73	.4	5.6	1	3
December	2.67	.5	4.7	3	2
Year	42.85	30.1	56.4	12	3

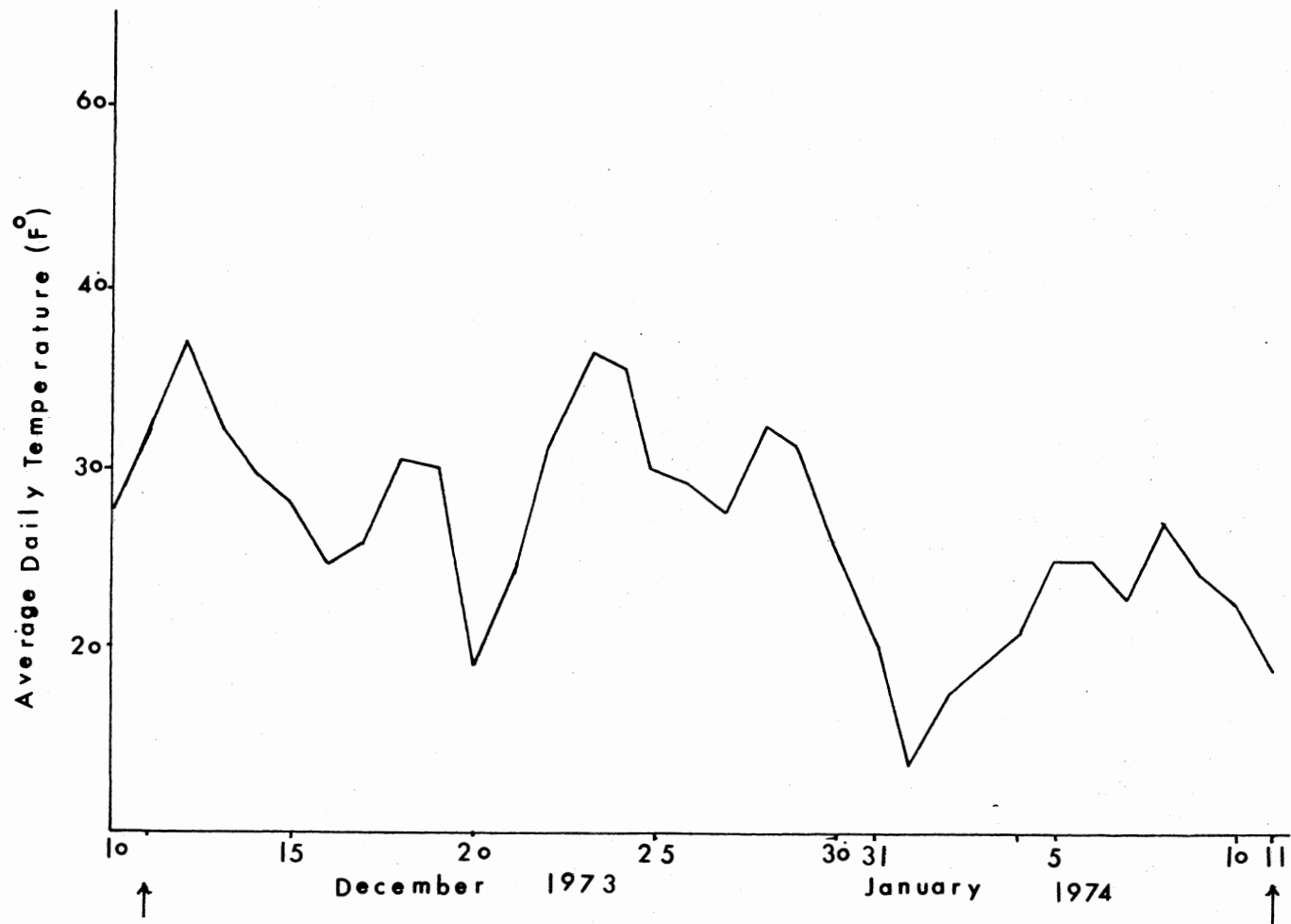


Figure 2 - Ranges of Average Temperature of Subscene Study Area for the Month LANDSAT Imagery and Skylab Photography Were Taken (Data obtained from Commerce Climatological Reports.)

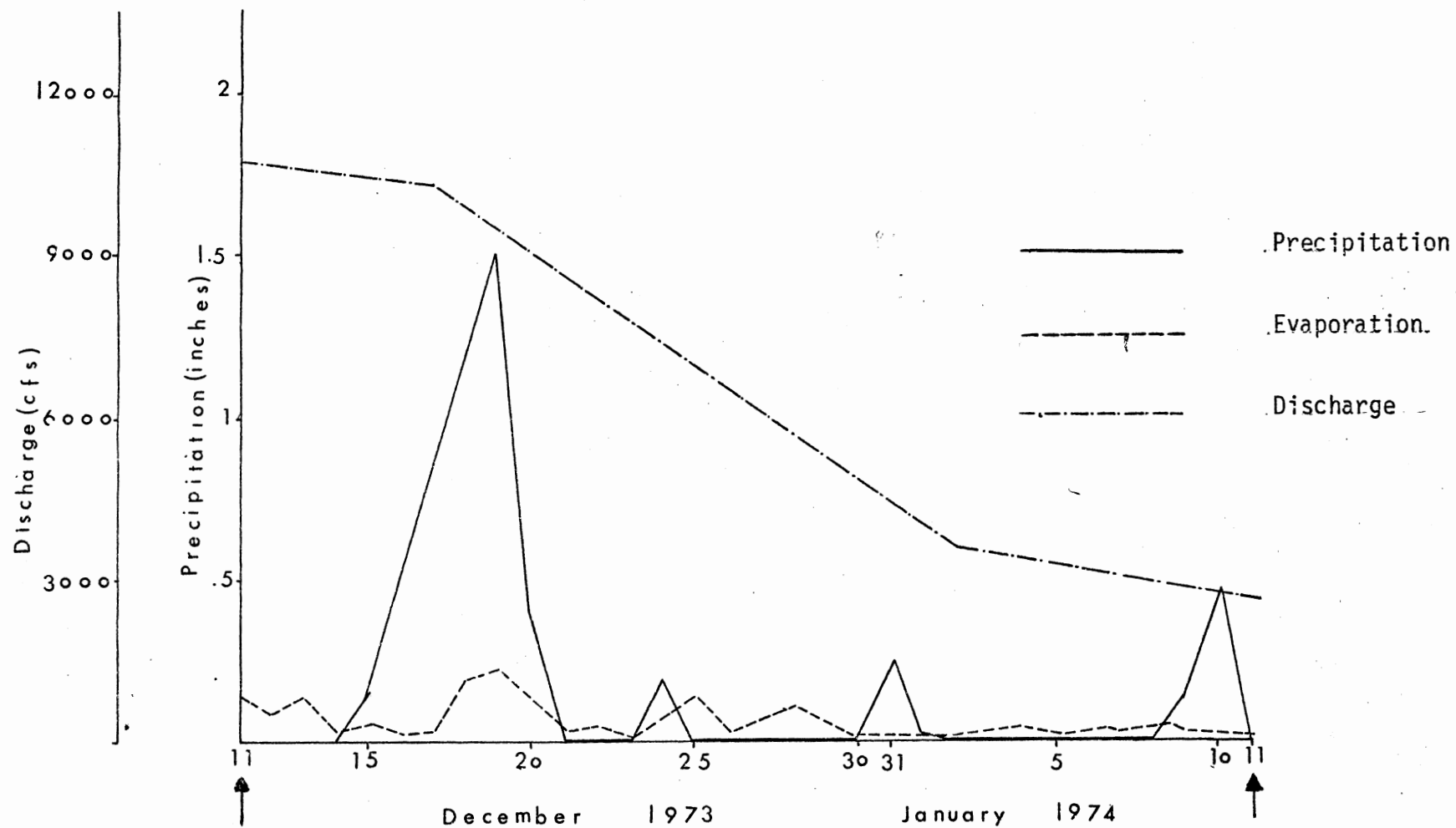


Figure 3 - Hydrograph of Daily Precipitation, Evaporation, and Discharge of Subscene Study Area for the Month LANDSAT Imagery and Skylab Photographs Were Taken (Data obtained from Commerce Climatological Reports.)

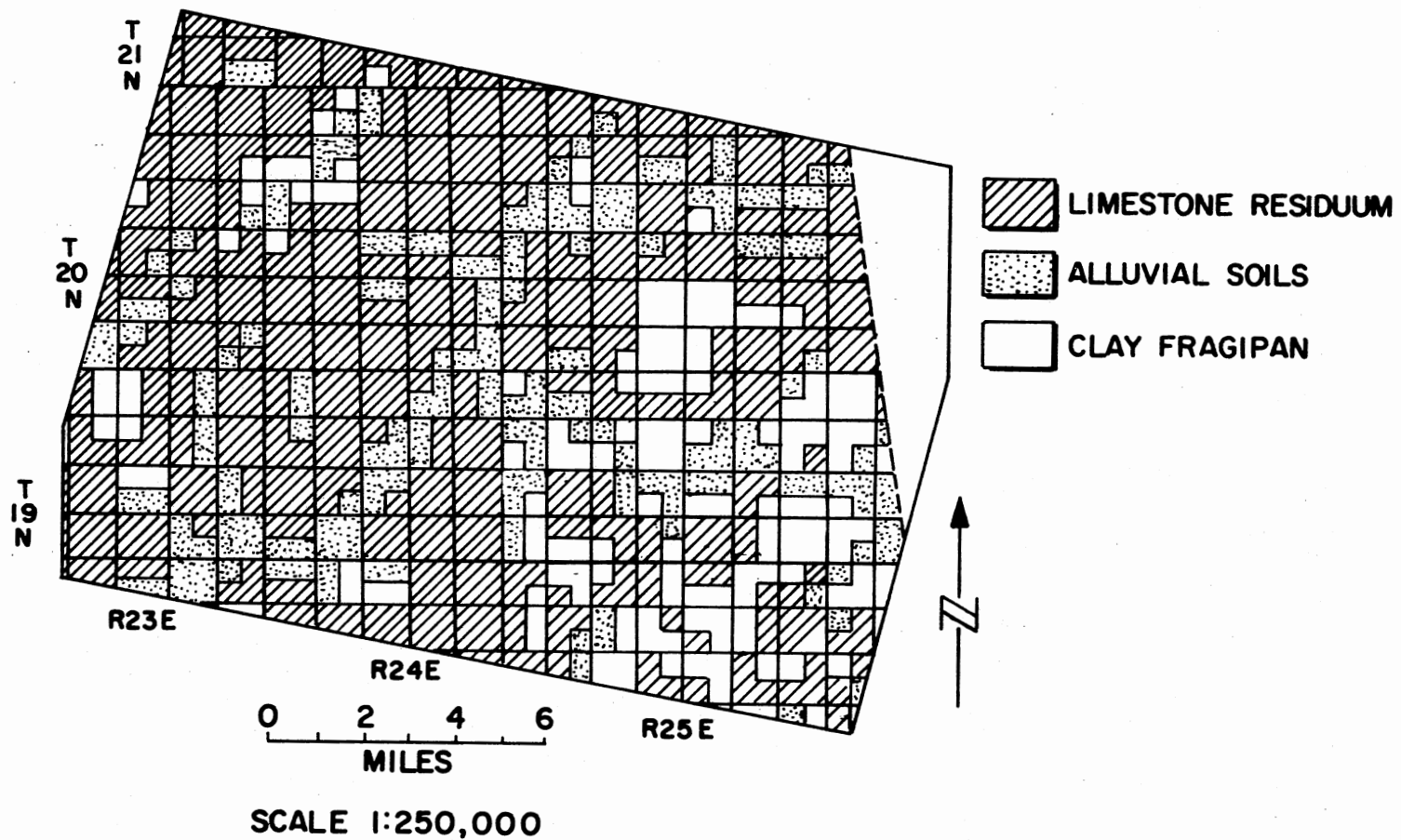


Figure 4 - Soil Map of the Subscene Study Area  
 (Data obtained from U.S. Soil Conservation Service Soil  
 Reports, 1965, 1970)



### Fragipan Soils

Fragipan soils are generally characterized by Jay and Locust soils in Delaware and Cherokee Counties. They consist of Capitinal silt loam with one to three percent slopes, Jay silt loam with zero to two percent slopes and Locust cherty loam having one to three percent slopes. In Adair County, the soil consists of Dickson silt loam with one to three percent slopes and Dickson cherty silt loam with zero to three percent slopes. Fragipan soils comprise about 12 percent of the subscene study area.

### Limestone Residuum Soils

Limestone residuum soils were developed from limestone characterized by a granular structure. This soil group occupies approximately 66 percent of the subscene study area. The soils group generally consists of Bodine, Craig, and Soyn series in Adair County, and of Baxter, Clarksville, Eldorado, and Newtonia series in Cherokee and Delaware Counties. The Bodine and Craig series extend over a wide area of the Ozark plateau in the southern part of the area. The Bodine series is typically very cherty or stony, acidic, and characterized by very steep to some gentle slopes. The Baxter series is formed from cherty limestone, and in some parts it consists of deep loamy soil with gentle to medium slopes. The Clarksville series is characterized by medium to steep slopes and has a stony and cherty medium-textured soil.

### Land Use

Land use in the thesis area was studied with the aid of an aerial

photograph mosaic for 1972, at a scale of 1:62500. Dense woodland, sparse woodland, crop lands, residential areas, pipelines, and highways were discernible on the mosaic. The land use map is shown in Figure 5. It was prepared utilizing the mosaic and using a one-quarter section (one quarter of one square mile) grid.

The forest areas are densely or sparsely wooded and comprise 54 percent of the subscene study area. Forests are found primarily in the hilly regions. Valleys generally have been cleared for grazing. Approximately 45 percent of the area is used for agriculture; residential areas occupy less than one percent of the study area. The towns of Watts and Kansas are the major residential areas. The Flintridge area supports trees and wild life, and is considered by many to be one of the more scenic areas in Oklahoma with exceptional recreational potential. Thus, the quality of ground water in this area is highly dependent upon the policies of these towns.

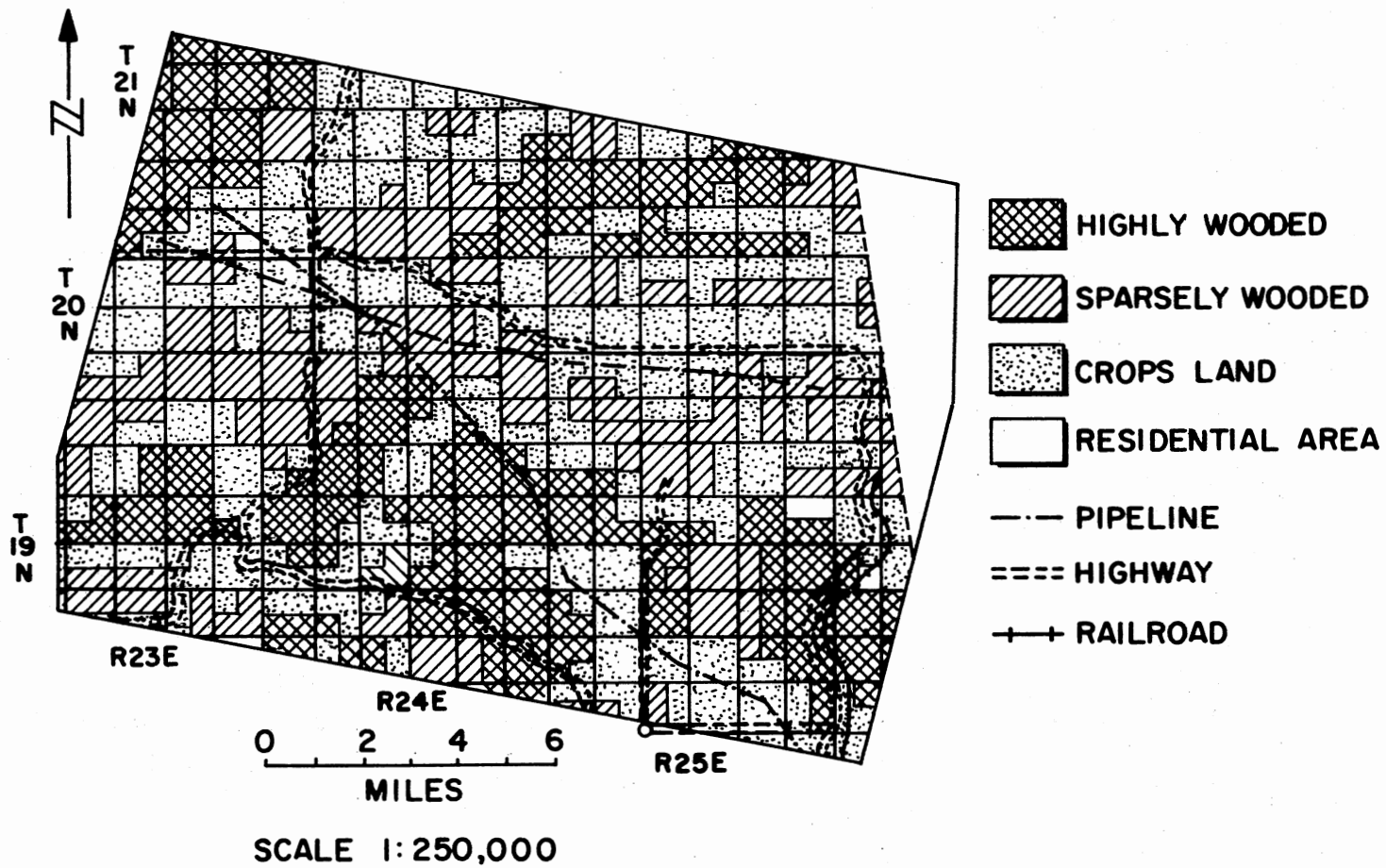


Figure 5 - Land Use Map of the Subscene Study Area.  
 (Data derived from an aerial photograph mosaic.)

## CHAPTER III

### GEOLOGY AND HYDROGEOLOGY

#### Physiographic Setting

The study area is part of the Ozark uplift. The Ozark uplift has been well described by Taff (1905), Snider (1915), Huffman (1951, 1958), and Watts (1977). It is a broad asymmetrical dome with an area of approximately 40,000 square miles in Missouri, Arkansas, and Oklahoma. The Ozark uplift is divided into three physiographic areas--the Salem platform, the Springfield structural plain, and the Boston Mountain plateau (Fig. 6). The study area is located in the Springfield structural plain. The area is a deeply dissected plateau and is underlain largely by chert and limestone of Osagean age (the Boone Formation). The upland surface of the Boone Formation is dissected by deep, V-shaped stream valleys. The drainage is joint controlled within this area.

The Boston Mountain plateau extends also into northeastern Oklahoma (Fig. 6), including the southern part of Adair and Cherokee Counties, the northern part of Sequoyah and the northeastern part of Muskogee Counties. The Boston Mountain area forms a narrow belt of rugged topography. The area is divided into prominent fault blocks flanked by northeast-southwest trending faults and characterized by steep escarpment faces and gentle dip slopes. Major drainages are

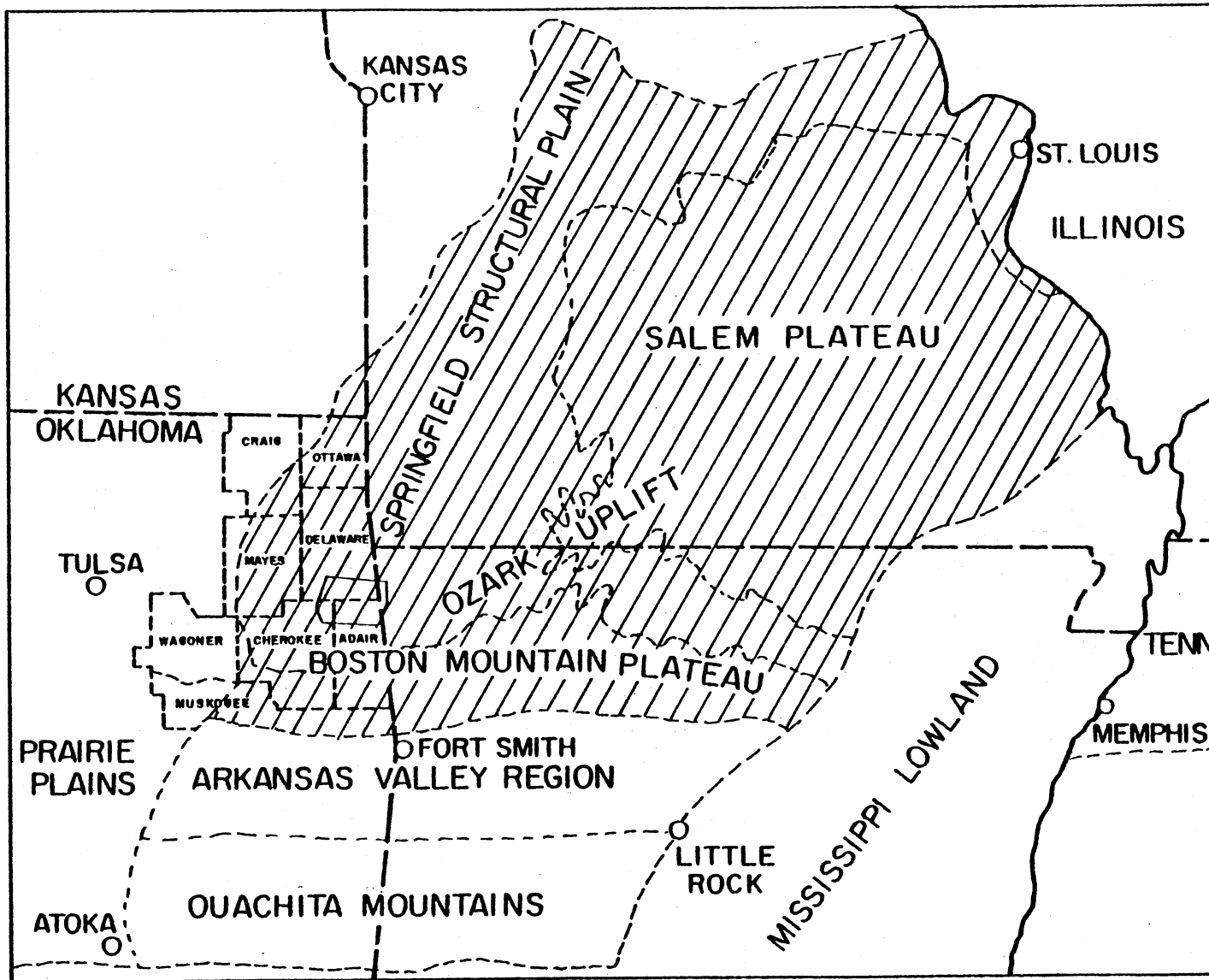


Figure 6 - Physiographic Provinces of the Ozark Uplift and Adjoining Areas (after Huffman, 1951)

developed in the softer shale and limestone (Huffman et al., 1958) parallel to the faults within this area.

### Stratigraphy

Rocks exposed in the Ozark region of Oklahoma range from the Cotter dolomite of lower Ordovician age to the Atoka sandstone of the middle Pennsylvanian age. Sedimentary rocks of Ordovician age include the Cotter dolomite, Burgen sandstone, and Tyner Formation. The Chattanooga shale is upper Devonian-lower Mississippian in age. Typical exposures occur on Flint Creek in Section 20, Twp. 20 North, Range 24 East. The Mississippian system is represented by the Boone, Moorefield, Hindsville, and Fayetteville Formations. A general description of the stratigraphic column is presented in Figure 7. Detailed characteristics of the formations which occur in the subscene study area are described in Appendix A. A generalized geologic map of the subscene study is shown in Figure 8.

### Regional Structure

The northeast-southwest trending faults and folds in northeastern Oklahoma conform with the elongation of the Ozark uplift. The alignment of these linear features is parallel to the axis of the Ozark uplift. The general regional dip of 25-50 feet per mile is interrupted by these linears. Faulting is most evident in the Boston Mountain plateau in Adair and Cherokee Counties.

Structural development of northeastern Oklahoma was associated with the growth of the Ozark geanticline, which was active during the Paleozoic Era. Huffman et al. (1958) described and listed the major

SYSTEM	SERIES	FORMATION	LITHOLOGY	THICKNESS	THICKNESS	
				(feet) Regional Area	(feet) Subscene Area	
PENNSYLVANIAN	Desmoinesian	McAlester	Dark gray-black, fissile, sh with three coals & underclays & basal Warner sandstone	50-150	0	
		Hartshorne	Conglomerate, coal, sh. & silt	0-50	0	
	Atokan	Atoka	Marine and non-marine sandstones and shales with occasional limestone beds. Units thin northward by convergence and overlap	0-600	0	
	Morrowan	Bloyd	Blue-gray, unevenly bedded limestone interbedded with gray, fissile shale. Absent north of T19N	0-200	0	
		Hale	Massive, blue-gray, sandy limestone	0-150	0	
MISSISSIPPIAN	Chesterian	Pitkin	Gray-blue limestone. Thin to extinction in T19N, R19E	0-80	0	
		Fayetteville	Black, fissile, shale with thin interbedded blue-black limestone	15-185	0-10	
		Hindsville	Gray limestone	0-48	0-7	
	Meramecian	Moorefield	Siltstone, shale, and limestone	0-100	0-18	
	Osagean	Boone	Keokuk	Massive, white to tan fossiliferous chert and dense blue limestone	0-250	?
			Reeds Spring	Blue-white to tan, thin bedded chert with beds of blue-gray, finely crystalline limestone	0-175	100-125
			St Joe	Gray limestones & green calcareous shale	0-70	5-70
DEV.	Kinderhookian	Chattanooga	Black, fissile, shale (Noel) & basal sandstone (Sylamore)	0-88	35-88	
	Ulsterian	Sallisaw	Brown, calcareous sandstone	0-25	0	
Frisco		Gray limestone	0-8	0		
SIL.	Niagaran	St. Clair	Pinkish-white limestone	0-155+	0	
		Sylvan	Yellow-brown, platy shale	0-35	0	
ORDOVICIAN	Cincinnatian	Fernvale	Gray limestone	0-25	0	
		Fite	Gray limestone	0-8	0	
		Tyner	Green shales & thin beds of buff sandy dolomite	0-90	0-<40	
	Champlainian	Burgen	White to yellow, hard massive sandstone with beds of dolomite & green shale	0-100+	0-100+	
		Canadian	Cotter	Gray to buff, finely crystalline, thick-bedded, dolomite	85-125	>13
	PRECAMBRIAN		Spavinaw	Red, coarse-grained granite	unknown	subsurface

Figure 7 - Stratigraphic Column for the Regional and Subscene Areas  
(from Watts, 1977)

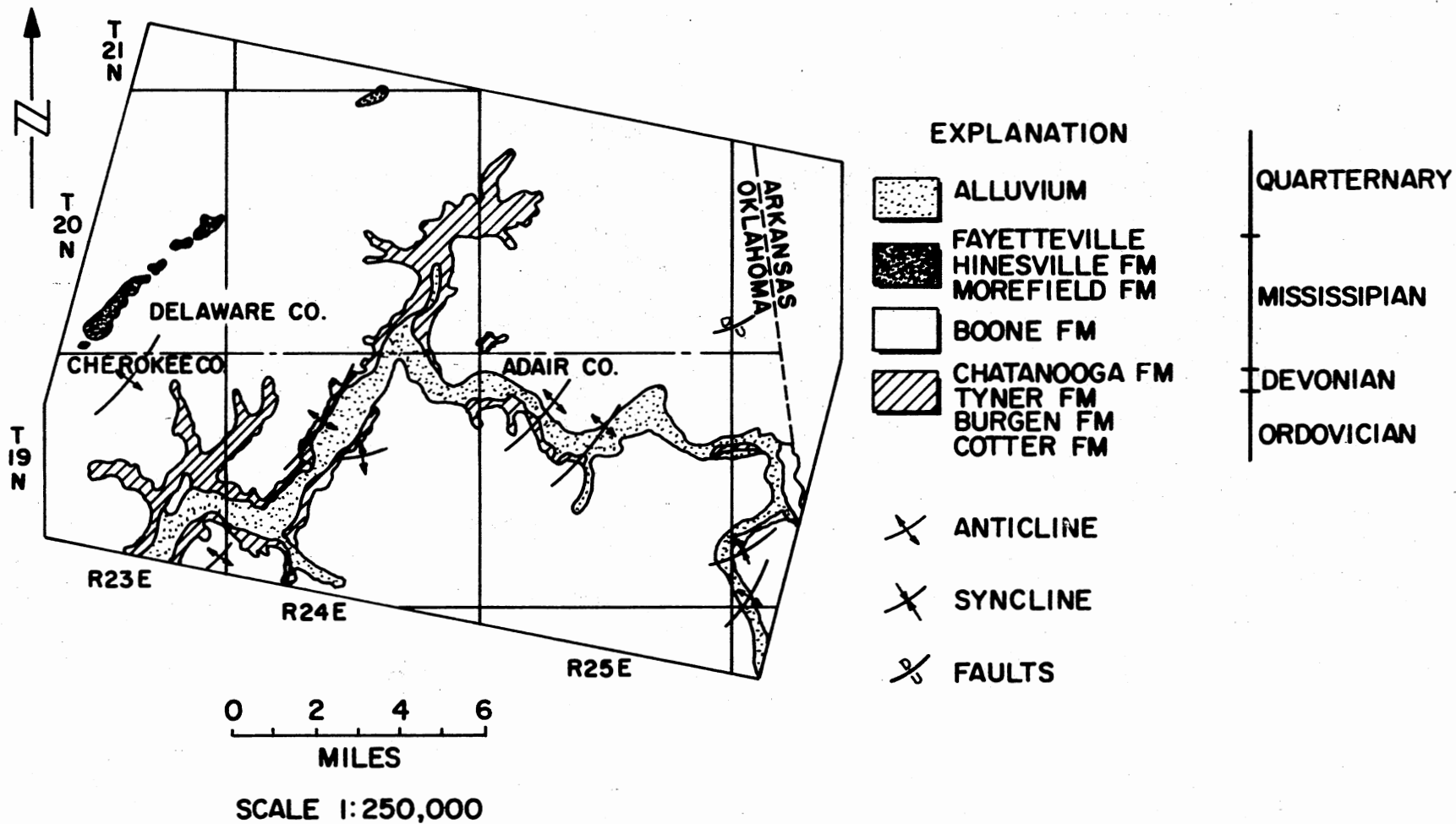


Figure 8 - Generalized Geologic and Structural Map of the Subscene Study Area, Delaware, Cherokee, and Adair Counties, Oklahoma (after Watts, 1977)



faults, folds, and joints. The structural features of the regional study area are shown in Figure 9.

## Ground Water

### Source and Movement

The occurrence of ground water in the subscene study area is associated directly with precipitation, rock type, permeability of soil, storage capacity, and particularly geologic structure. The average precipitation is approximately 42 inches; hence, about 2200 acre-feet fall on each square mile each year. Recharge to ground-water storage is estimated to be about 110 to 550 acre-feet (5 percent to 25 percent of precipitation).

The Keokuk and Reed Springs Chert and the St. Joe Limestone Member of the Boone Formation form the major shallow aquifer of the area. The Boone Formation is shown on the geologic map in Figure 8 to occupy approximately 80 percent of the study area. The fractured Keokuk and Reed Spring Cherts underlie the limestone residual soil, which is highly permeable; hence, most of the water percolates downward through fractures and associated solution cavities. Because the aquifer is underlain by the relatively impermeable Chattanooga shale, the ground-water movement is restricted to the Boone Formation and is forced to move laterally to adjacent drainages. High well yields and the occurrence of springs in the Boone Formation are evidence of the occurrence and movement of ground water in the fractured medium of the Boone Formation. In some areas, the spring flow can be traced to solution cavities developed from limestones below the Keokuk and Reed Springs Formations.

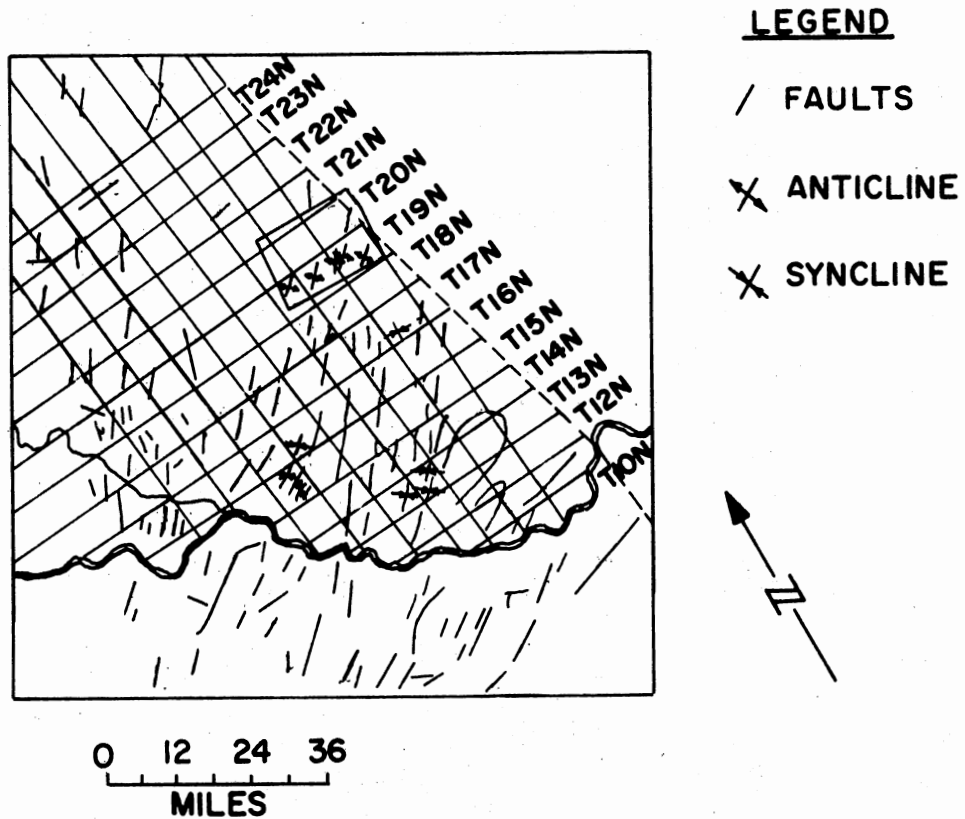


Figure 9 - Generalized Structural Map of the Regional Study Area, northeastern Oklahoma (after Marcher, 1969)

The relationship between rainfall and ground-water levels is shown in Figure 10. An increase of ground-water level as a response to rainfall is also described by Marcher (1969). Flood plains alluvium and terrace deposits are other important sources of water in the study area. Yields up to 650 gpm have been reported from wells located in Section 3, Twp. 19 North, Range 24 East.

#### Ground-water Quality

Chemical quality analyses of ground water in the subsurface area included the evaluation of 55 analyses of water samples from wells and springs; twelve of these samples were collected by the writer. The balance were from unpublished data of the Oklahoma State Department of Indian Health Services, Water Quality Division. The analyses included total hardness, total dissolved solids, sulfate, chloride, nitrate, pH, sodium, potassium, calcium, bicarbonate, carbonate, and specific conductance. A summary of the chemical analyses is presented in Tables III and IV. In general, the chemical quality of the Boone Formation is good, but there are some values that indicate high total hardness and high nitrate concentrations. Nitrate concentrations over 45 ppm and total hardness which exceed 180 ppm are considered to be hazardous for drinking water according to the U. S. Public Health Service drinking water standards (Marcher, 1969). Water from alluvium and weathered chert is softer than water from deeper wells in contact with the Chattanooga Formation. Total hardness is caused by compounds of calcium and magnesium bicarbonate. Water that has a hardness of less than 60 ppm is rated soft.

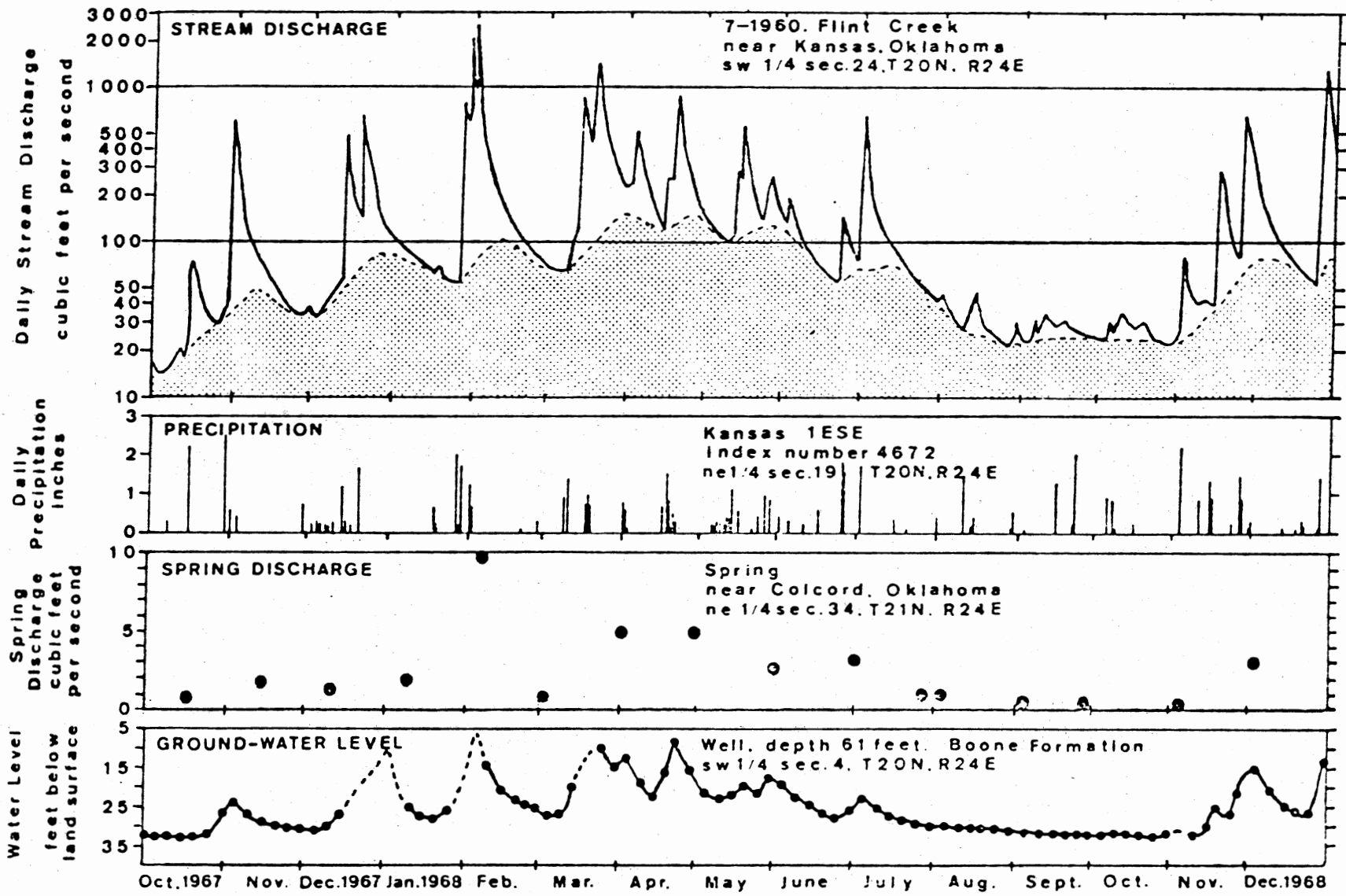


Figure 10 - Graphs of Mean Daily Stream Discharge, Daily Precipitation, Monthly Springflow, and 5-day Ground-water Level for the Subscene Study Area (from Watts, 1977)

TABLE III  
SUMMARY OF CHEMICAL ANALYSES OF WATER SAMPLES

	Concentration (ppm)			Number of Analyses
	Maximum	Mean	Minimum	
Iron	1.0	0.21	0.05	26
Chloride	118.0	20.77	0.2	42
Sulfate	125.0	21.91	0.2	40
Nitrate	32.0	2.68	0.1	28
Hardness	1000.0	156.13	5.0	42
Total dissolved solids	388.0	222.67	83.0	28
pH	7.9	7.56	6.7	15
Well yield (gpm)	650.0	76.50	1.0	20

TABLE IV  
SUMMARY OF CHEMICAL ANALYSES OF WATER SAMPLES  
COLLECTED BY THE AUTHOR

	Concentration (ppm)			Number of Analyses
	Maximum	Mean	Minimum	
Iron	0.09	0.033	0.01	12
Chloride	32.7	13.5	6.0	12
Sulfate	8.8	1.8	0.0	12
Nitrate	67.8	11.99	4.4	12
Hardness	145.0	78.33	35.0	12
Total dissolved solids	268.0	138.33	62.0	12
pH	8.0	7.47	7.1	12
Sodium	37.3	7.75	2.0	12
Magnesium	5.9	1.57	0.6	12
Calcium	54.6	25.69	10.4	12
Potassium	2.39	0.48	0.07	12
Bicarbonate	142.7	80.20	10.8	12

## CHAPTER IV

### ANALYSIS OF LINEARS FOR POLLUTION SUSCEPTIBILITY AND WATER QUALITY

The first Earth Resources Technology Satellite (ERTS-1) was placed in a near-polar orbit at an altitude of 920 km in July, 1972. ERTS-2 was launched in January, 1975, to replace ERTS-1. Subsequently, the acronym was changed to LANDSAT A and B. LANDSAT C was launched in March, 1978. The LANDSAT satellites are equipped with a multispectral scanner (MSS) from which analog data are transmitted to receiving stations throughout the world. Data are digitized and transferred to tape as well as recreated on photographs through a series of filters. The multispectral data represent four electromagnetic bands: green (band 4, 0.5 to 0.6 micrometers); red (band 5, 0.6 to 0.7 micrometers); near-infrared (band 6, 0.8 to 0.8 micrometers), and second near-infrared (band 7, .8 to 1.1 micrometers). The imagery covers approximately 132,225 square miles. These satellites have provided coverage over the earth every 18 days; they orbit the earth fourteen times a day from north to south.

In addition, Skylab data were used for comparison with the LANDSAT data. Four Skylab manned-space craft missions were launched; the fourth Skylab-4 passed over the study area on January 11, 1974. Photographic cameras equipped with six high precision f/1.8 lenses having a 15.2 cm focal length were used to provide multispectral coverage. The

following wavelength frequencies were used in this study: A2 (.8-.9 micrometers), A3 (.5-.88 micrometers), A4 (4.-.7 micrometers), A5 (.6-.7 micrometers), and A6 (.5-.6 micrometers).

"Linear" refers to any line "that is structurally controlled, including any alignment on separate photographic images, such as stream beds, trees, or bushes that are so controlled" (Chavez, 1971). In this study, the term "linear" applies to any line, straight or slightly curved.

### Previous Investigations

Several studies have been made for investigation of linear features in the study area and adjacent and other areas.

#### Local and Adjacent Areas

Watts (1977) correlated the trend of linears with the joint orientation measured in the field within this study area. Aerial photographs were also analyzed for drainage orientation. The comparison of the trends of LANDSAT linears with the joint and drainage orientations were presented as histograms and are shown in Figure 11. He concluded that the great proportion of LANDSAT linears were representative of joint controlled drainage segments having a northeast-southwest orientation.

Wagner, Steel, MacDonald and Coughlin (1976) evaluated the linears discernible on aerial photographs taken in north central Washington County, Arkansas. Water samples were collected from wells and springs located on linears and off linears. The samples were analyzed for sodium (Na), potassium (K), calcium (Ca), magnesium (Mg), strontium (Sr), iron (Fe), copper (Cu), zinc (Zn), nitrate (NO<sub>3</sub>), and phosphate



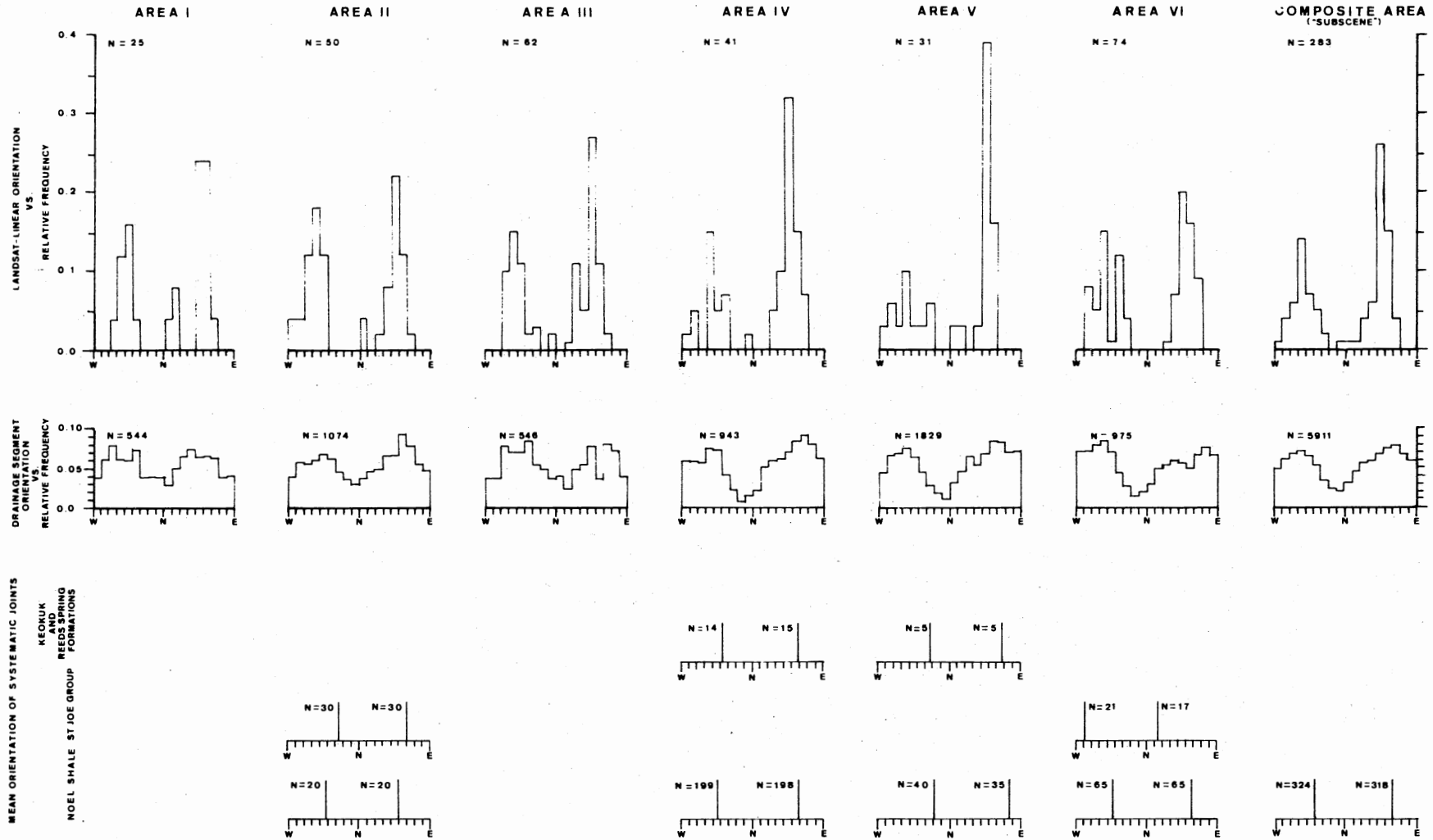


Figure 11 - Orientation Histograms of LANDSAT Linears, Drainage and Joints in the Subscene Area. The letter "n" refers to the sample size. All data are plotted in ten degree classes (from Watts, 1977)

( $PO_3$ ). The Boone Formation was also the principal aquifer in that area. Samples from wells located on linears indicated that 79 percent of the wells had surface contamination (inorganic and organic), and 57 percent of the wells were shown to have fecal contamination. Data from the deep wells which were not located on linears were used to show that

. . . the water quality in a carbonate terrain can be adversely affected by linears by allowing more ready access of surface contamination from bacteria and nitrate (p. 444).

### Other Areas

El Shazley et al. (1974) applied LANDSAT imagery for purposes of distinguishing linear features in the Aswan area of Egypt. They mapped several major structural features which had not been previously mapped.

Ebtehadj (1973) used LANDSAT imagery to map geologic features of Iran. He reported a number of large-scale faults which had not been shown on existing geologic maps. He also discovered a number of small lakes and streams which had not been previously identified.

Russell et al. (1974) applied LANDSAT imagery and high altitude color infrared photography in the investigation of the Eastern Interior coal basin. They reported subsurface fractures could be delineated due to subtle differences in the overlying glacial till.

Anguswantana et al. (1974) used LANDSAT imagery for discrimination of drainage, faults, fractures, and folds in Thailand. They recognized several kinds of faults in the area, including normal faults, thrust faults and wrench faults.

Chavez (1976) used LANDSAT multispectral scanner (MSS) digital image data to enhance linears recognized on nondigital LANDSAT products in southwestern Jordan and adjacent areas. He used two types of

image corrections for the image enhancement processing. He also interpreted numerous linears of various dimensions that were not identified on standard (MSS) image products. Several of these linears were proven to be previously unmapped faults.

### Data Processing

The data processing used in this investigation is presented in Figure 12. Photographic products and digital data from LANDSAT A were used in conjunction with Skylab-4 S190A photographs.

#### Standard LANDSAT Imagery

The LANDSAT-1 multispectral scanner (MSS) imagery is acquired in four separate spectral bands of 4, 5, 6, 7. The images of black and white paper print of negative and positive band 7 and false color composite (FCC) for December 11, 1978, were used in this investigation.

#### Computer-enhanced Digital Data

The computer processing techniques of this study were derived from LANDSAT A multispectral scanner data for scene E-1506-16263 (December 11, 1973). The detailed analysis of digital data was described by Watts (1977, pp. 41-52). The same processing techniques were used in this study except that eight lines per inch were used for the gray-scale printer output instead of six lines per inch; thus, the white spaces around the pixels would be reduced. Steps used in processing the multispectral data is summarized in Figure 12.

Briefly, the first step was subscene location (Fram). This program copies the location of the corresponding coordinates of the study

# DATA PROCESSING

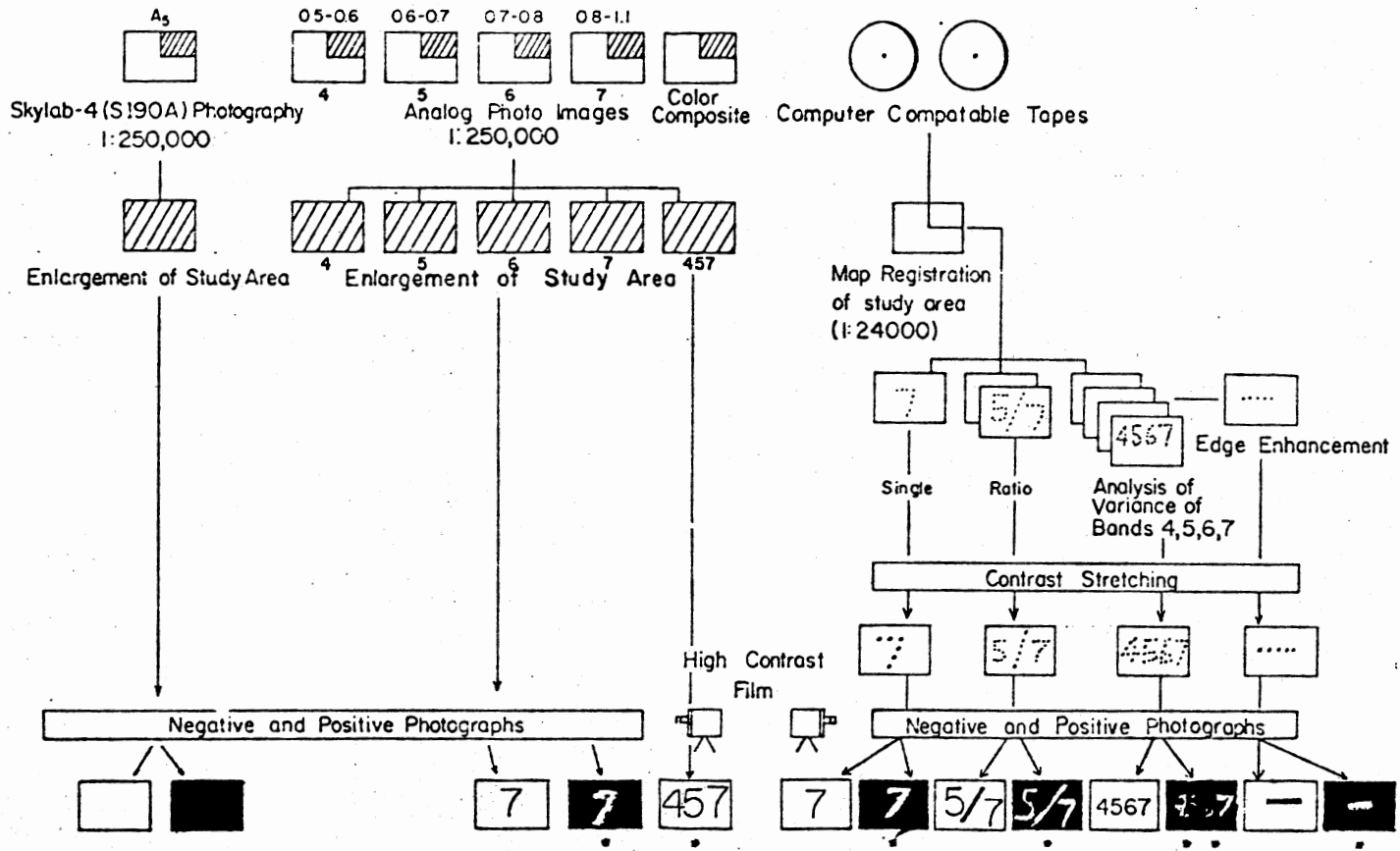


Figure 12 - Data Processing Chart

area from an entire scene (over seven million data points) onto tape storage. A column width of 500 pixels (east-west) and line width of 250 pixels (north-south) was desired for the study area. In processing LANDSAT data, some scenes may exhibit horizontal lines (banding). The "smooth" program compensates for this banding effect with no significant data alteration. The data set should be smoothed after it is located (Fram). The "registration" and "transformation" programs were used to orient the data spatially to standard map coordinates and to correct the stretch caused by the nature of the multispectral scanner, rotation of the earth, and movement of the satellite in orbit. The "registration" program computes point coefficients which are derived from two sets of point coordinates. The old points are taken from the Army topographic map and the corresponding points are obtained from a smoothed gray scale map of the subscene study area. Use of Band 7 is preferred for this purpose. The computer enhancement techniques used on the digital data of this study were ratioing of the multispectral bands and principal components 1 and 2 (PC-1, 2). The latter consists of the following programs of COVAR, EIGEN, PRICOM. These programs are also described by Watts (1977).

#### Skylab-4 190A Photographs

Earth Resources Experiment Package (EREP) photographs were used for regional study and small scale linear discrimination in this study. Skylab-4 190A (SL-4) coverage of northeastern Oklahoma occurred over the study area on January 11, 1974. The percentage of cloud cover during its mission over the area was zero, so cloud-free photographs of the area were obtained. The Skylab photographs are not scanner products

but rather actual photographs taken with a Hozebloc camera using filters for different spectral frequencies; SL-4 represents A1 to A6. These photographs provide a higher resolution than scanner imagery can provide, therefore high resolution satellite photographs can be compared with LANDSAT multispectral imagery at the same scale (1:250,000) and of compatible electromagnetic frequencies.

### Linear Evaluation Methods

The utility of Skylab photography was used for identifying large-scale linears in the larger study area. Linears mapped have a minimum length of approximately five miles and may be caused by topographic relief, textural contrast, alignments of drainage, and color contrast. The shadowing due to areas of high relief and low sun angle can cause enough contrast to enhance the linear topographic features. A linear map at a scale of 1:250,000 of the regional study was prepared from the linears exhibited on the Skylab image. The major structural feature of the area consists of faults, anticlines, synclines, and major physiographic features including the Salem platform, Springfield structural plain and Boston Mountain plateau. Linears within the smaller subscene area included both large and small-scale linears with a minimum length of a quarter of a mile, LANDSAT imagery photos, Skylab photos, and computer-enhanced. Digital maps were used to evaluate these linears within the study area. Photographic and digital products were photographed using 135 mm Kodachrome slide films. The slides were projected to a scale of 1:24,000 on a screen covered with tracing paper. The observed linears were drawn onto the tracing paper for each type of LANDSAT and Skylab product. The linear map of the standard LANDSAT

imagery (Band 7 and color) is shown in Figure 13. Linear maps for the computer-enhanced digital map and Skylab-4 black and white and color photographs are shown in Figures 14 and 15, respectively. Linear maps have been reduced to the scale of 1:250,000.

Most of the linear features are better defined by principal components one and two (PC-1 and PC-2) images of the multispectral (MSS) data. The landuse features such as pipelines, power lines, highways, and railroads were recognized and eliminated from the original linear features. The linears exhibited on the linear maps were used to prepare linear density maps derived from the standard LANDSAT Band seven and color imagery (Fig. 16), from computer-enhanced digital images (Fig. 17), Skylab-4 (Fig. 18), and from drainage density (Fig. 19). The linear densities were determined for each square mile by measuring the lineal scaled distance (feet) of all linears occurring within a single square mile. The lineal distances were classified into four classes showing relatively high and low fracture density. The four classes include the following lineal distance per square mile: 1 (0-1000 feet), 2 (1001-5000 feet), 3 (5001-10,000 feet), 4 (> 10,000 feet).

The linear density maps were used for comparison with each other and with a drainage density map. The drainage map was prepared from the Army topographic quadrangle map at the scale of 1:250,000. The comparison of LANDSAT linears with drainage are shown in Figure 20.

Maps showing the number of intersections were derived from linear maps by extending linears to one-fourth of their length. Intersections formed by the extended linears were counted for each square mile. These maps are shown in Figures 21, 22, and 23, for three types of imagery.

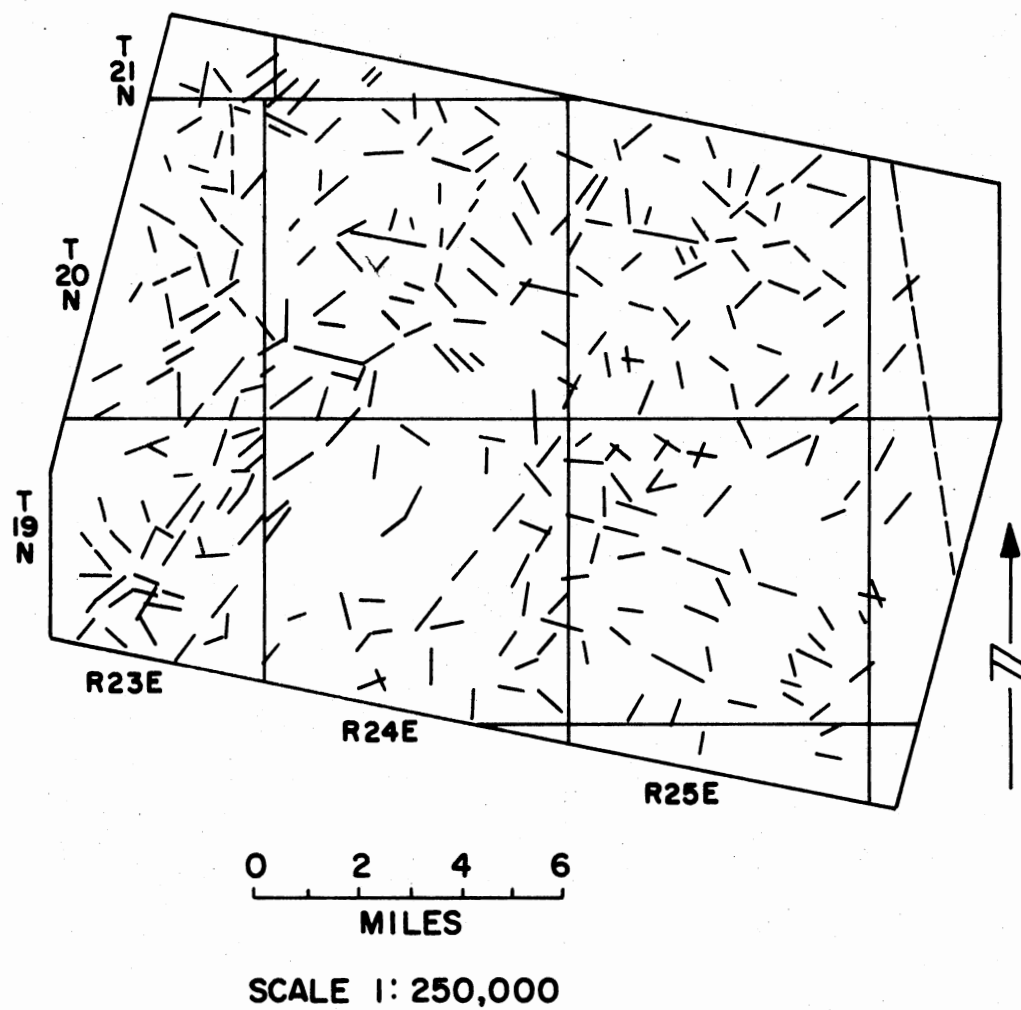


Figure 13 - Linear Map of the Subscene Study Area Derived From Standard LANDSAT Imagery (Neg. Band 7 and color composite)



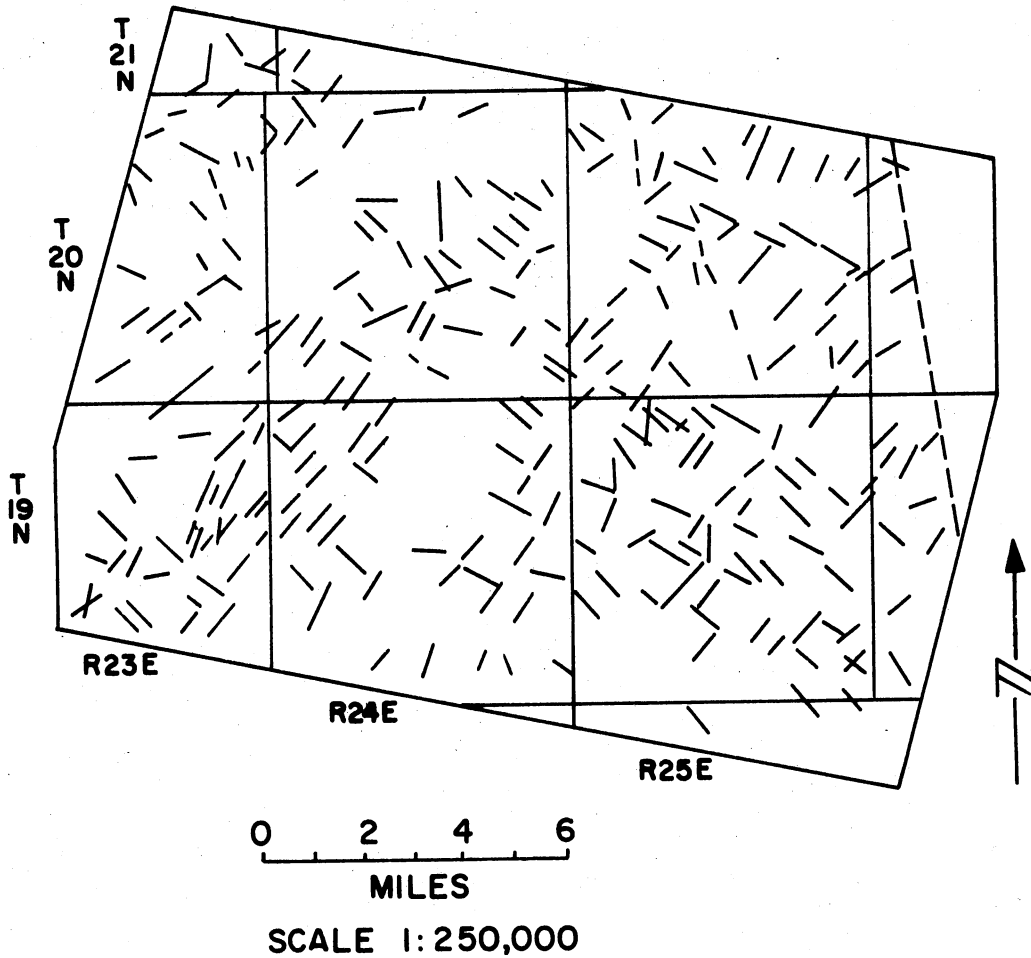


Figure 14 - Linear Map of the Subscene Study Area  
Derived From Computer-enhanced Digital  
Imagery (PC-1, 2)

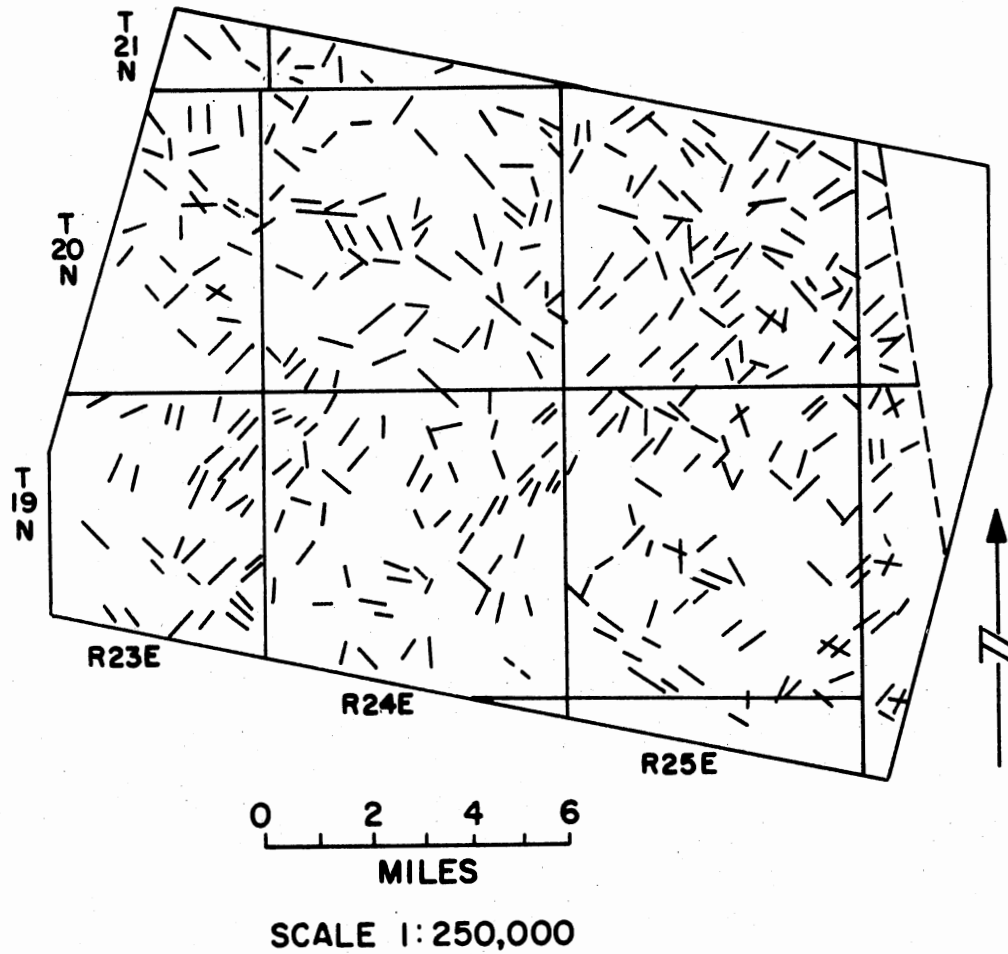


Figure 15 Linear Map of the Subscene Study Area  
Derived From Skylab-4 S190A Photography

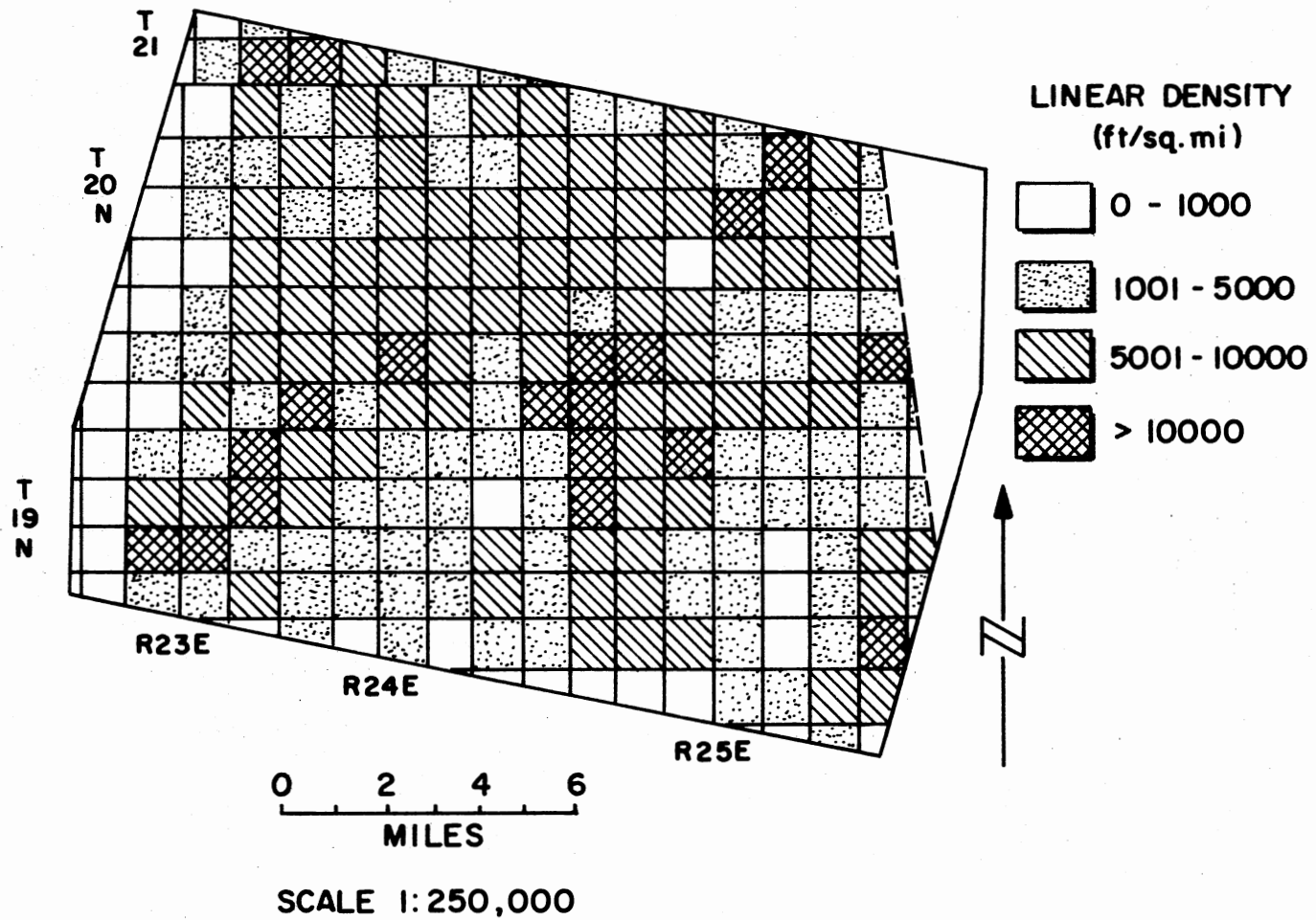


Figure 16 - Linear Density Map of the Subscene Study Area Derived From Standard LANDSAT Imagery (Fig. 13)

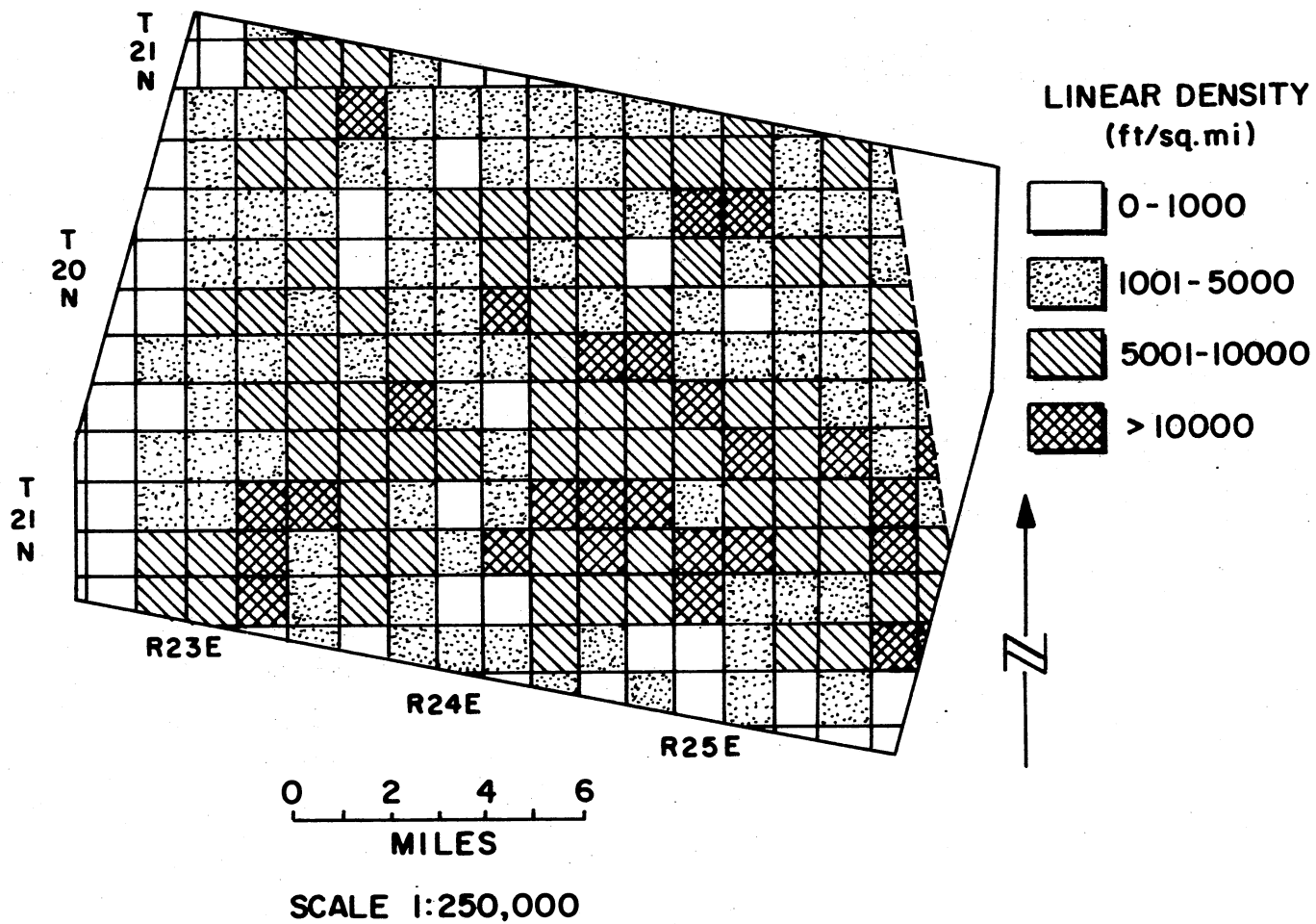


Figure 17 - Linear Density Map of the Subscene Study Area Derived From Digital LANDSAT Imagery (Fig. 14)

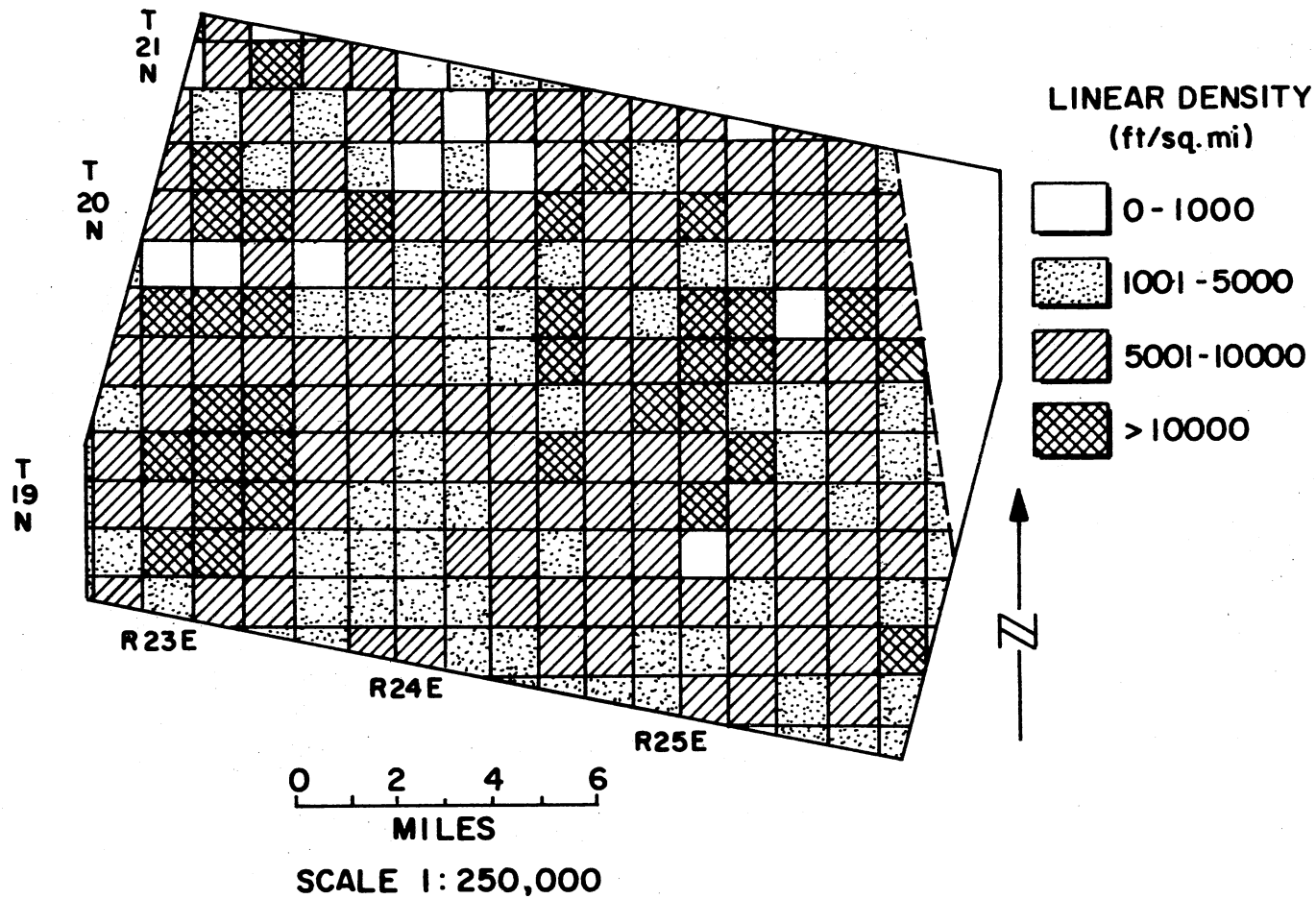


Figure 18 - Linear Density Map of the Subscene Study Area Derived From Skylab-4 Photography (Fig. 15)

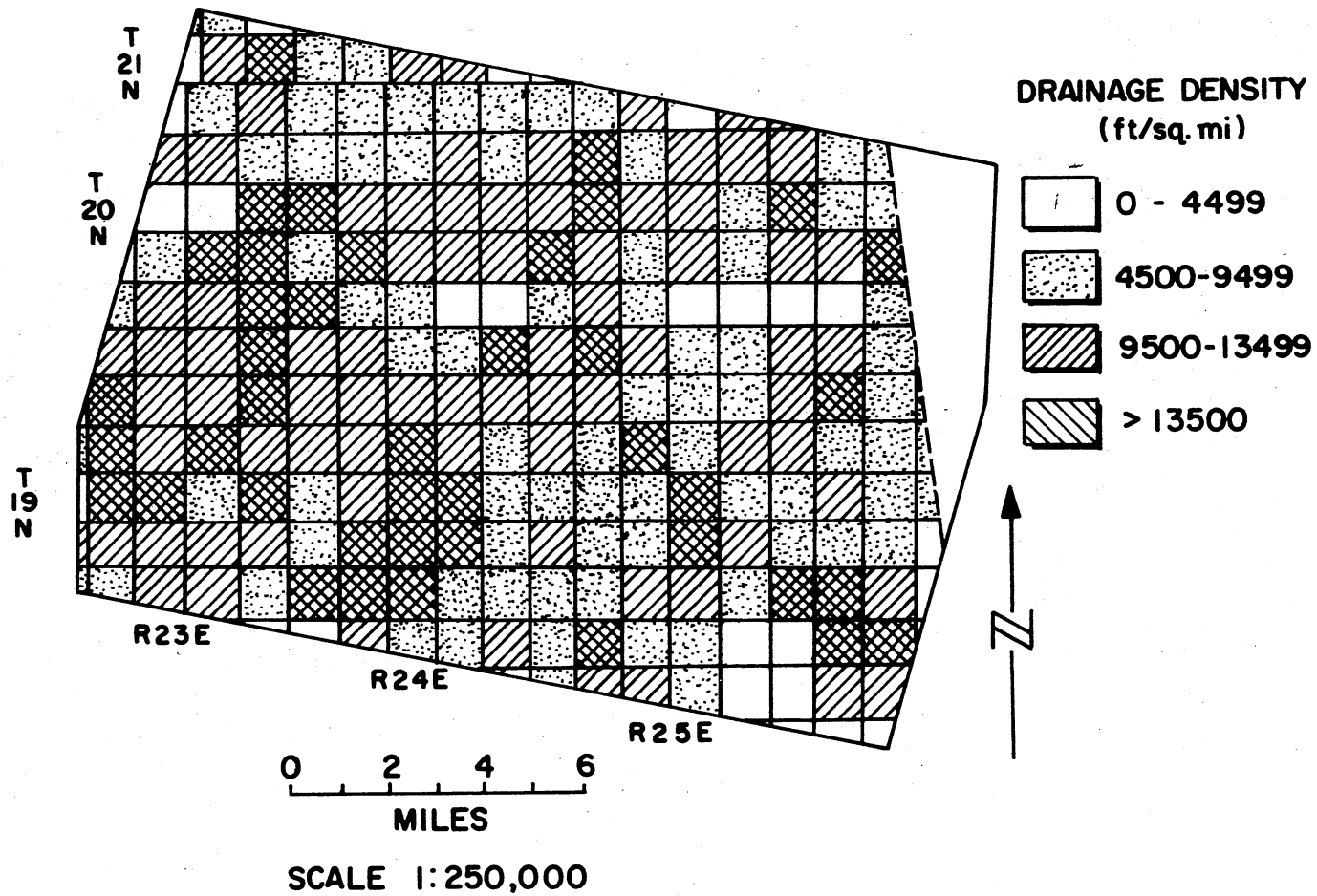


Figure 19 - Drainage Density Map of the Subscene Study Area

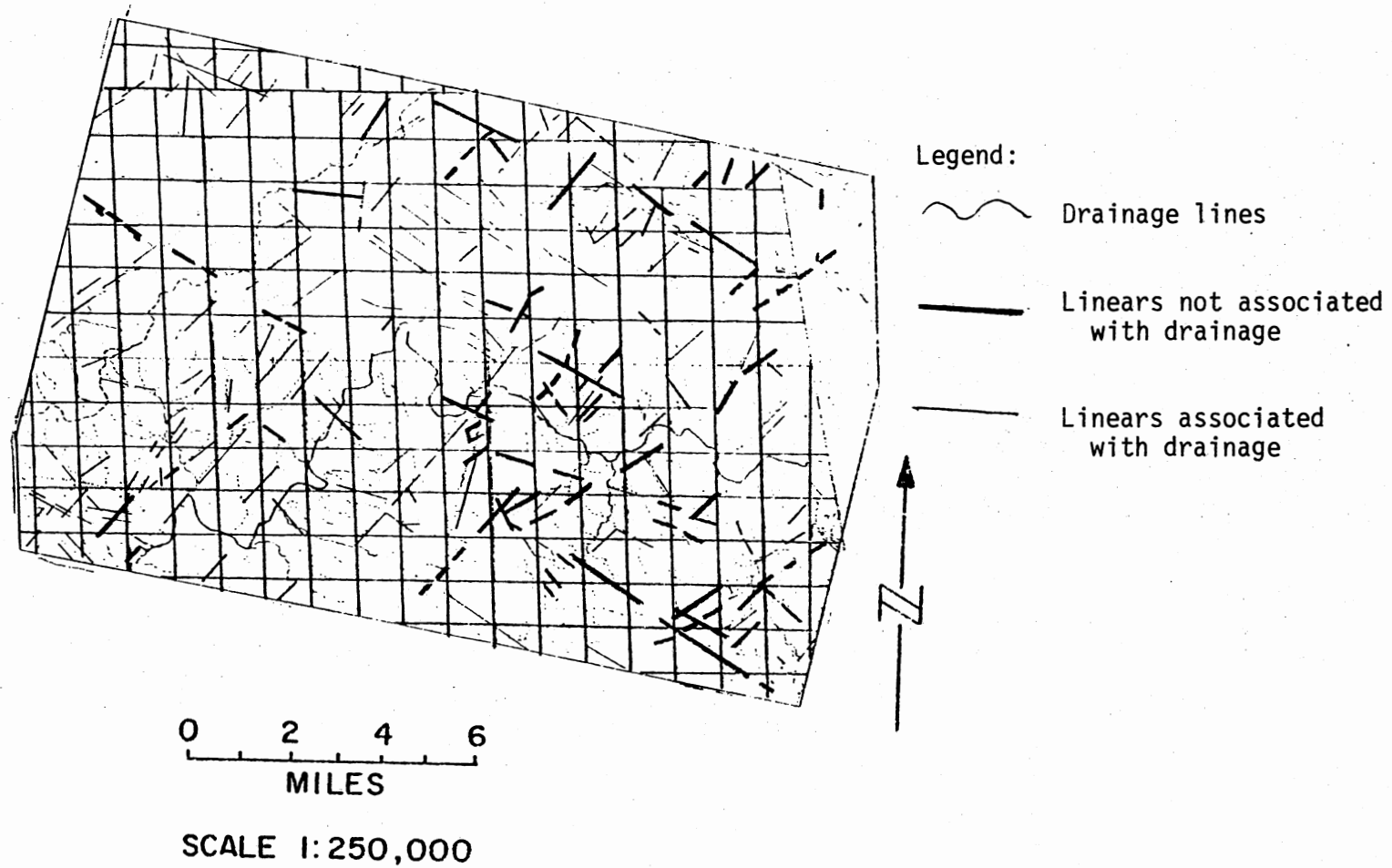


Figure 20 - Comparison of LANDSAT Linears With Drainage

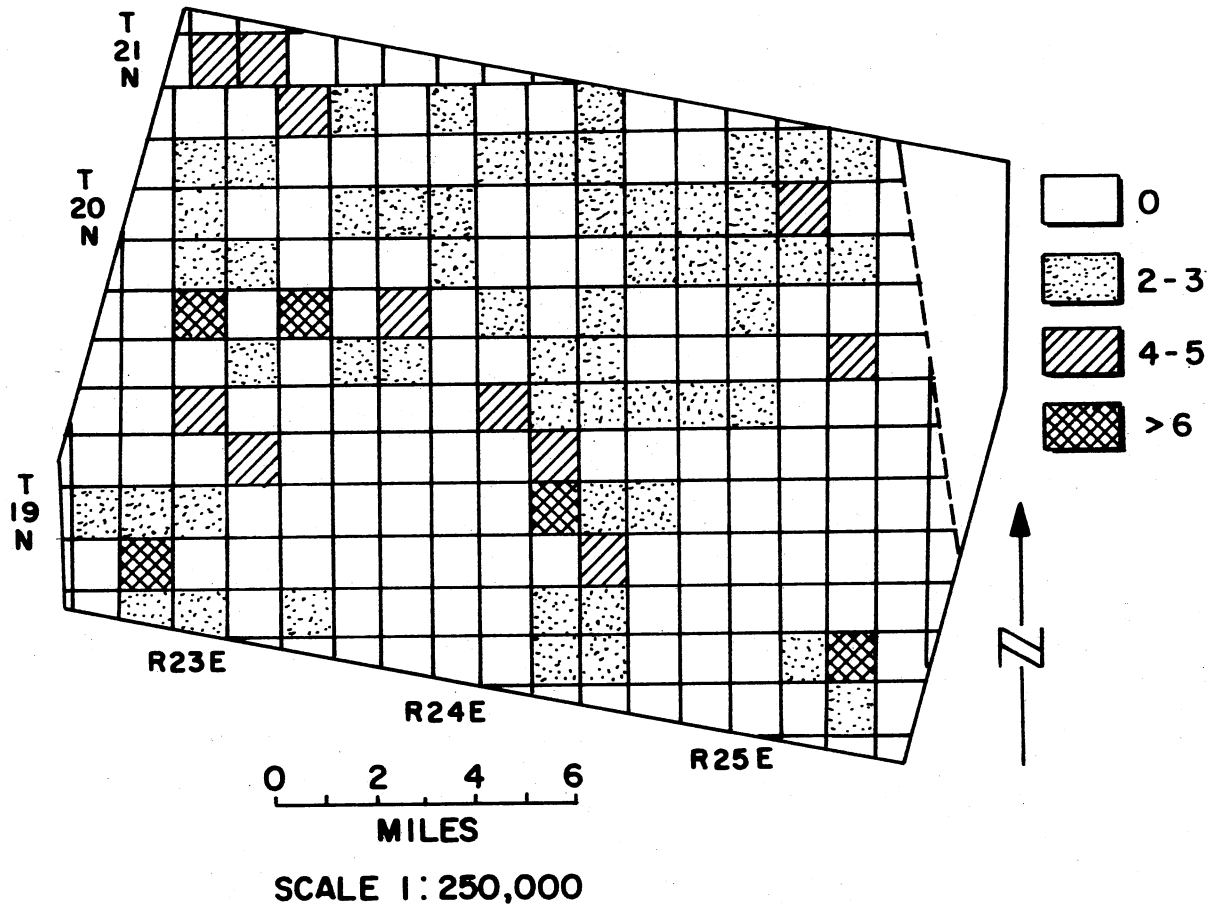


Figure 21 - Number of Intersections Map of the Subscene Study Area Derived From Standard LANDSAT Imagery Linears (Fig. 13)



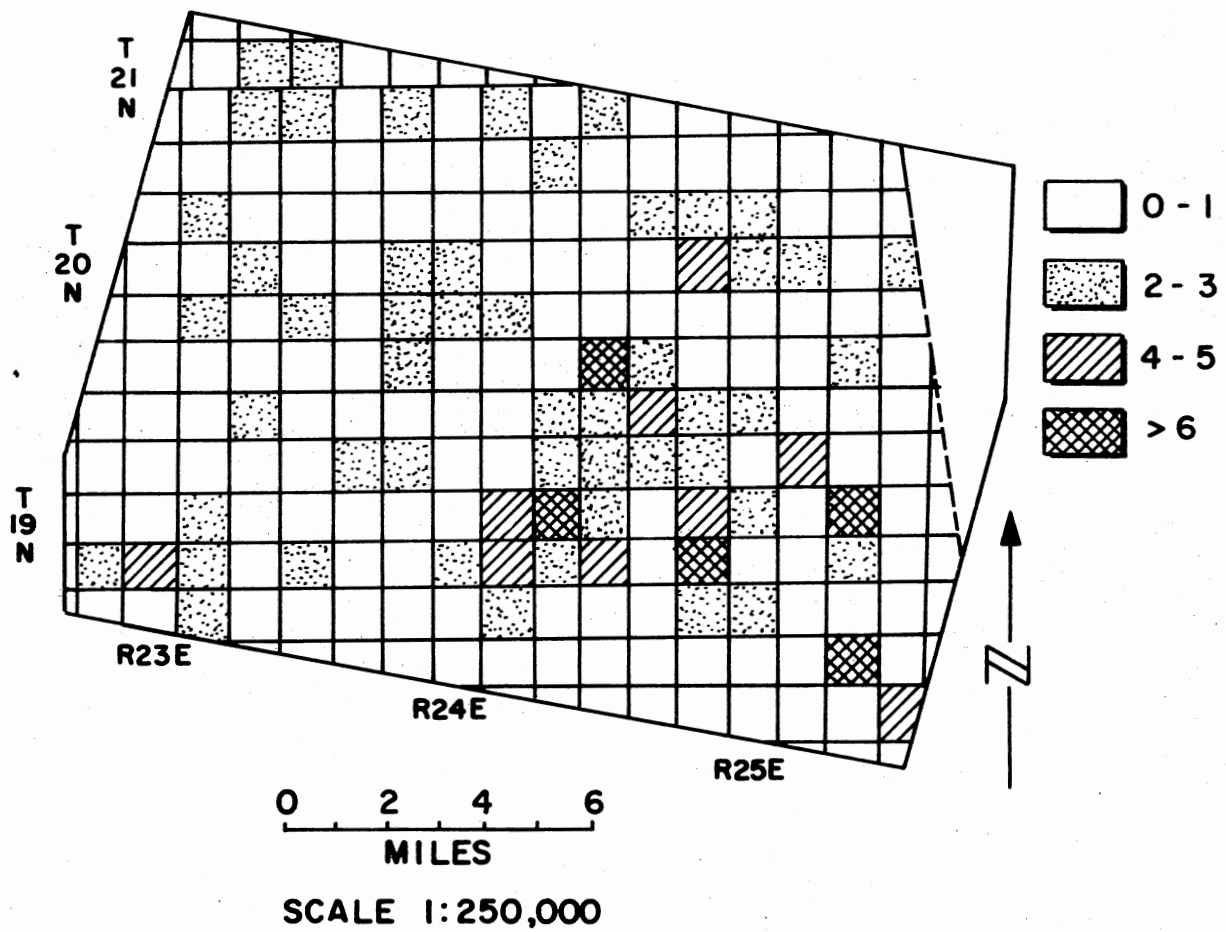


Figure 22 - Number of Intersections Map of the Subscene Study Area Derived From Computer-enhanced Digital Imagery Linears (Fig. 14)

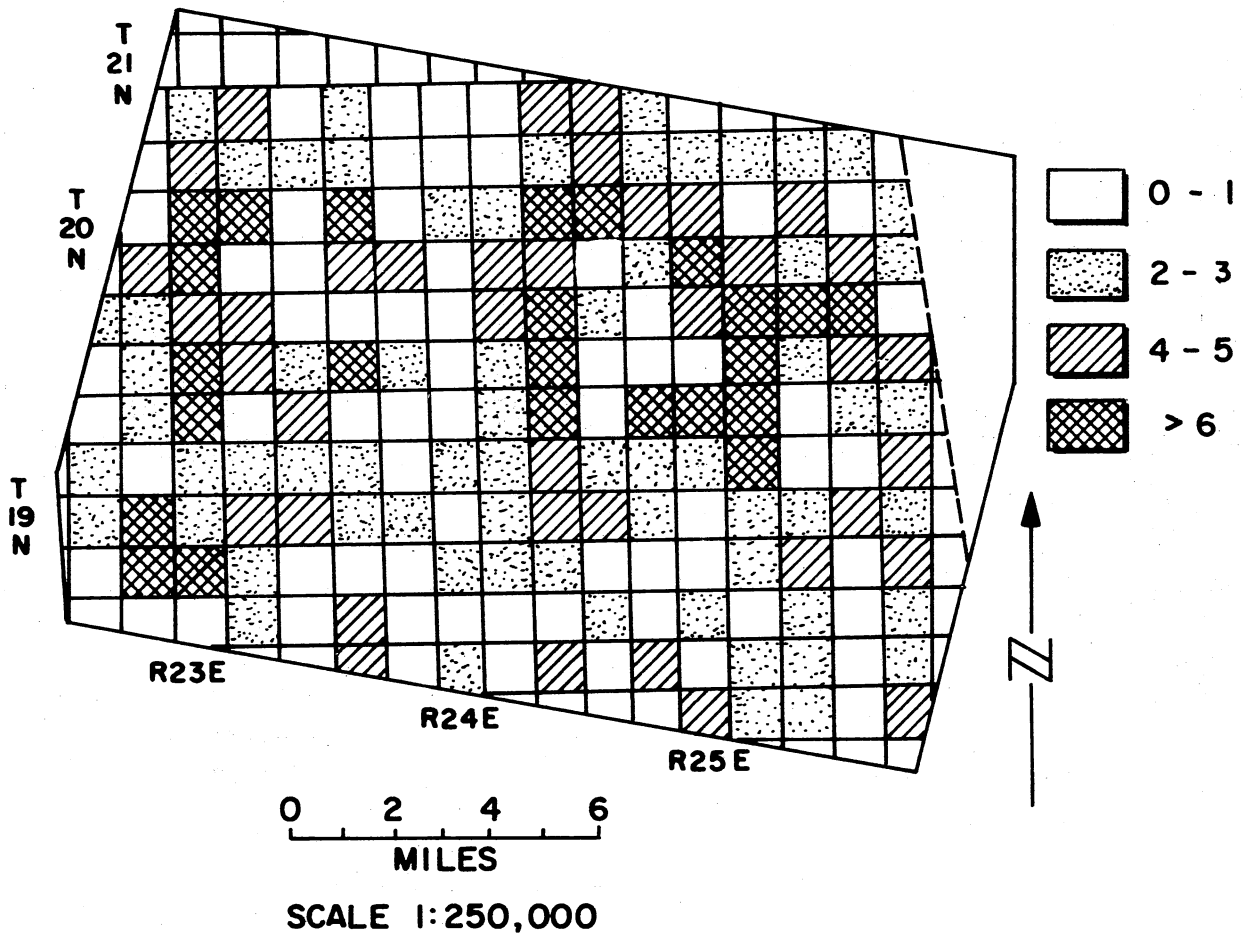


Figure 23 - Number of Intersections Map of the Subscene Study Area Derived From Skylab-4 Linears (Fig. 15)

### Linear Evaluation - Results

The linear density maps and maps showing the number of intersections per square mile are compared in Tables V and VI, respectively. Linear density maps derived from Band 7 Standard LANDSAT imagery and computer-enhanced digital maps correlated very well, but correlation between linear density maps derived from LANDSAT imagery and from Skylab photography were relatively poor. A higher fracture density can be noted on the linear maps derived from Skylab data. This conclusion is based on results summarized in Table V. The number of intersections derived from the Skylab data is significantly different from the number of intersections derived from the LANDSAT data. This can be noted in Table VI.

TABLE V  
COMPARISON OF LINEAR DENSITIES

Map Source	Linear Density	Linear Density* (ft/sq mi)				Total
		0-999 ft/mi <sup>2</sup>	1000-4999 ft/mi <sup>2</sup>	5000-999 ft/mi <sup>2</sup>	10,000 ft/mi	
Principal component (digital-enhancement)		12.5	37	38.5	12	100
Standard LANDSAT Imagery (Band 7)		10	39	41	10	100
Skylab (bxw, A <sub>5</sub> )		5	27	51	17	100

\*All values are in 100 percent.

TABLE VI  
COMPARISON OF NUMBER OF INTERSECTIONS

Map Source	Number of Inter- sections	Intersection Density* (No/mi <sup>2</sup> )				Total
		0-1	2-3	4-5	6>	
Standard LANDSAT Imagery (Band 7)		66.2	26.0	5.5	2.5	100
Principal component (digital-enhancement)		68.5	24.5	4.5	2.5	100
Skylab (bxw, A <sub>5</sub> )		40.5	31.5	16.5	13.0	100

\*All values in 100 percent.

A comparable correlation can be made for the maps showing the number of intersections per square mile. The map which shows the number of intersections derived from Skylab has a significantly greater number of intersections than noted on those derived from LANDSAT products.

#### Pollution Susceptibility

The pollution susceptibility of the area was evaluated using linear density maps--maps showing the number of intersections and available soil and land use information of the subscene study area. Maps showing linear densities, drainage density, and number of intersections were superimposed on soil maps. The levels of susceptibility range from the most susceptible to the least susceptible. These levels were identified as classes; classes 1 and 2 represent the most susceptible

level, and class 4 corresponds to the lowest level of susceptibility. Criteria for identification of pollution susceptibility classes are listed in Table VII. High linear density areas corresponding with the soil type of limestone residuum were considered most susceptible, and low linear density areas corresponding with clay fragipan were considered as least susceptible areas. The correspondence of alluvial soil with high and moderate density areas may be considered most susceptible or moderately susceptible, depending on the number of intersections. The pollution susceptibility maps of the subscene study area include those derived from standard LANDSAT imagery (Fig. 24), LANDSAT digital PC-1, 2 (Fig. 25), Skylab-4 (Fig. 26), composite LANDSAT digital imagery (Fig. 27), and from drainage density (Fig. 28).

There is a strong association between ground-water quality and pollution susceptibility of the area. Previously, Steel et al. (1976) reported the relation between high nitrate, potassium and phosphate concentrations with the wells located on linears identified on aerial photographs. High concentrations of nitrate were identified in wells located in Section 9, Twp. 20 North, Range 24 East; Section 4, Twp. 19 North, Range 25 East, and Section 32, Twp. 20 North, Range 25 East. These locations correspond to areas of (class 2) high susceptibility.

These pollution susceptibility maps show predictable levels of pollution susceptibility and recharge areas overlying the Boone aquifer adjacent to the Illinois River. The comparison of pollution susceptibility maps is shown in Table VIII. Levels of pollution susceptibility were similar for different map sources. However, exceptions can be noted. Skylab data provided a greater percentage of high susceptibility areas (classes 1 and 2); whereas the percentage of low susceptibility

TABLE VII  
 CRITERIA FOR IDENTIFICATION OF POLLUTION  
 SUSCEPTIBILITY CLASSES

Linear Density (ft/sq mi)	Soil Type	Pollution Susceptibility Classes
>10,000	limestone residuum	1
	alluvial soil	2
	clay fragipan	3
5,001-10,000	limestone residuum	2
	alluvial soil	2
	clay fragipan	3
1,001-5,000	limestone residuum	3
	alluvial soil	3
	clay fragipan	4
0-1,000	limestone residuum	3
	alluvial soil	4
	clay fragipan	4

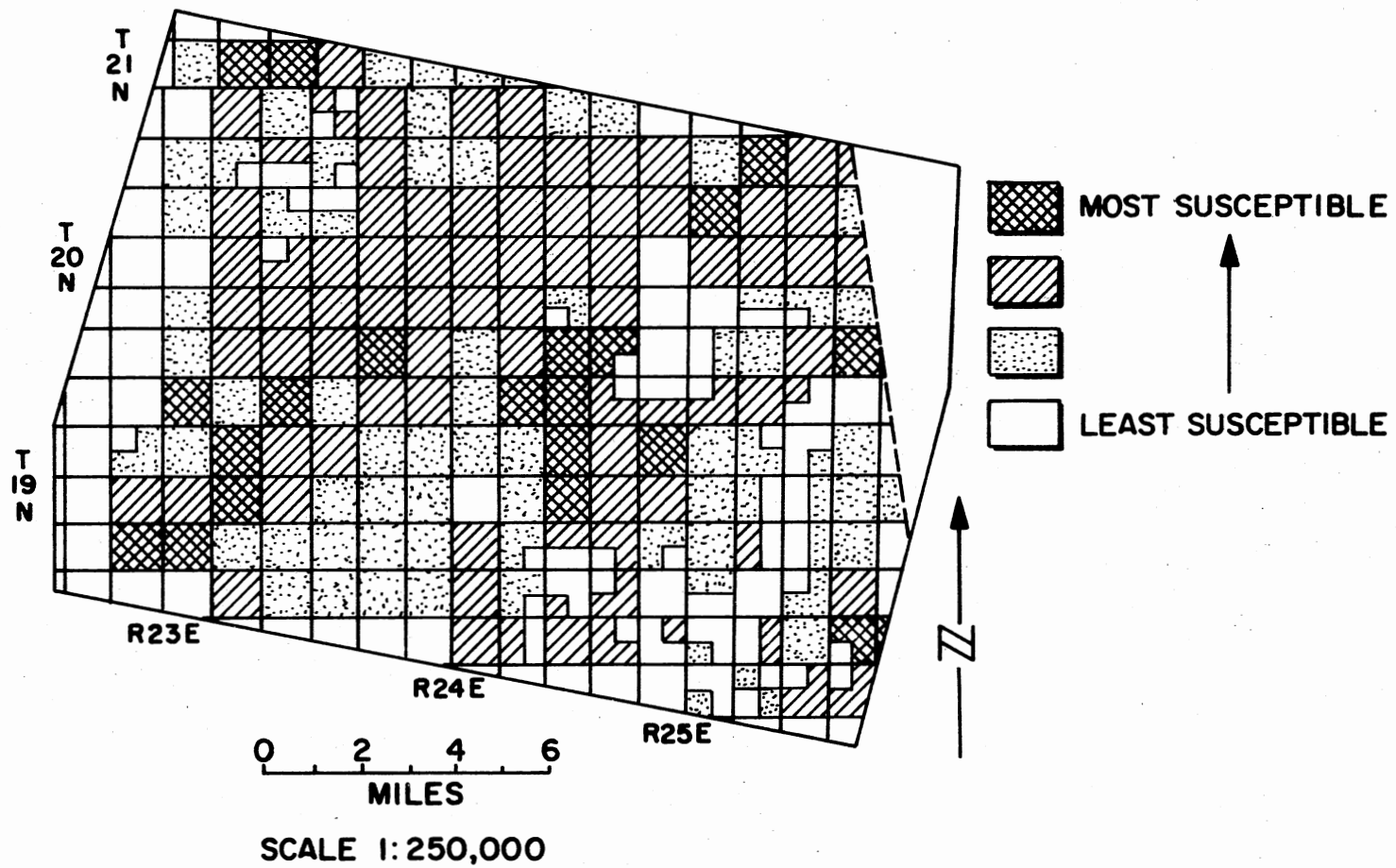


Figure 24 - Pollution Susceptibility Map of the Subscene  
 Study Area Derived From Standard LANDSAT  
 Photography (Neg. Band 7 and color com-  
 posite)

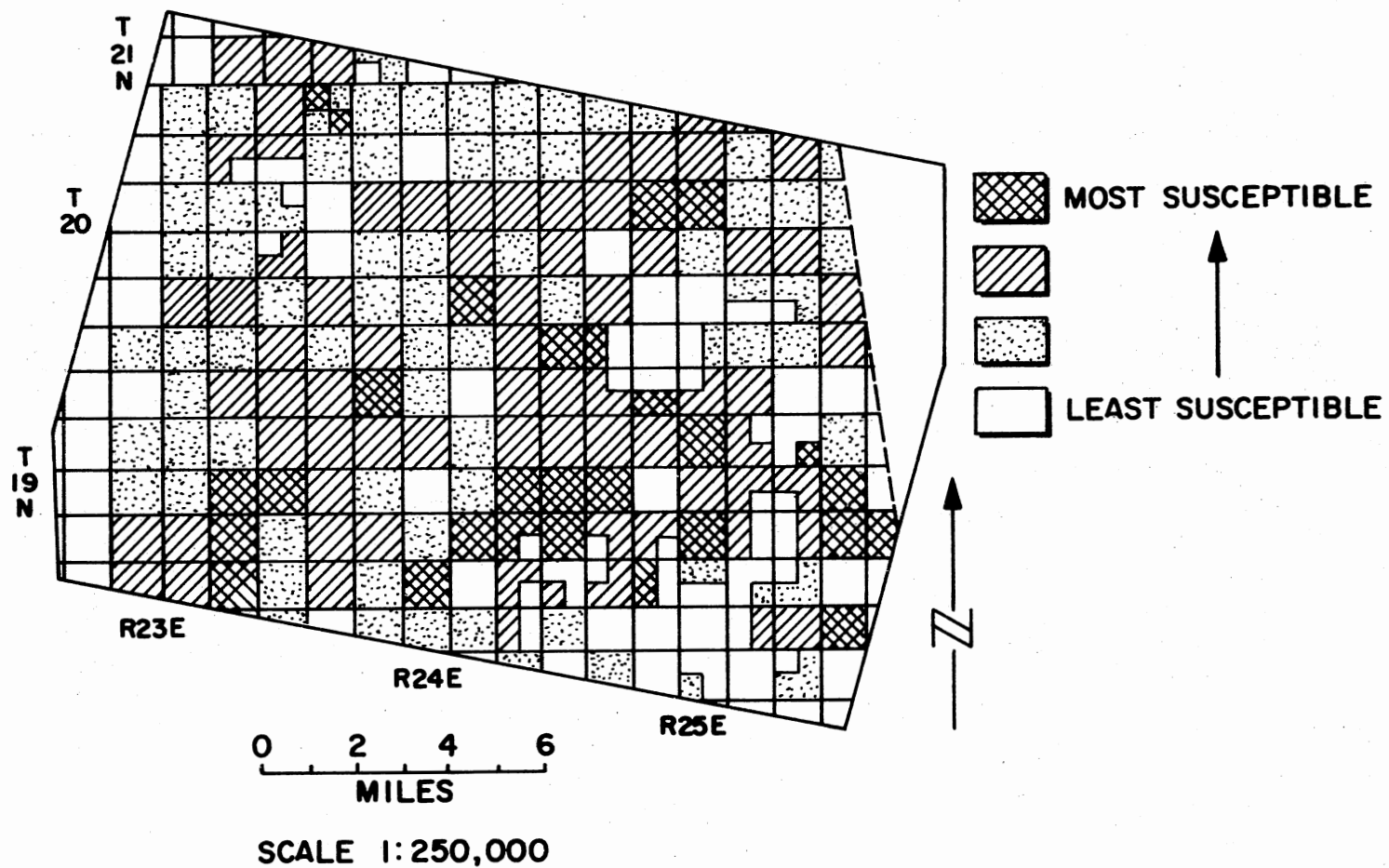


Figure 25 - Pollution Susceptibility Map of the Subscene Study Area Derived From Computer-enhanced Digital Imagery (PC-1, 2)



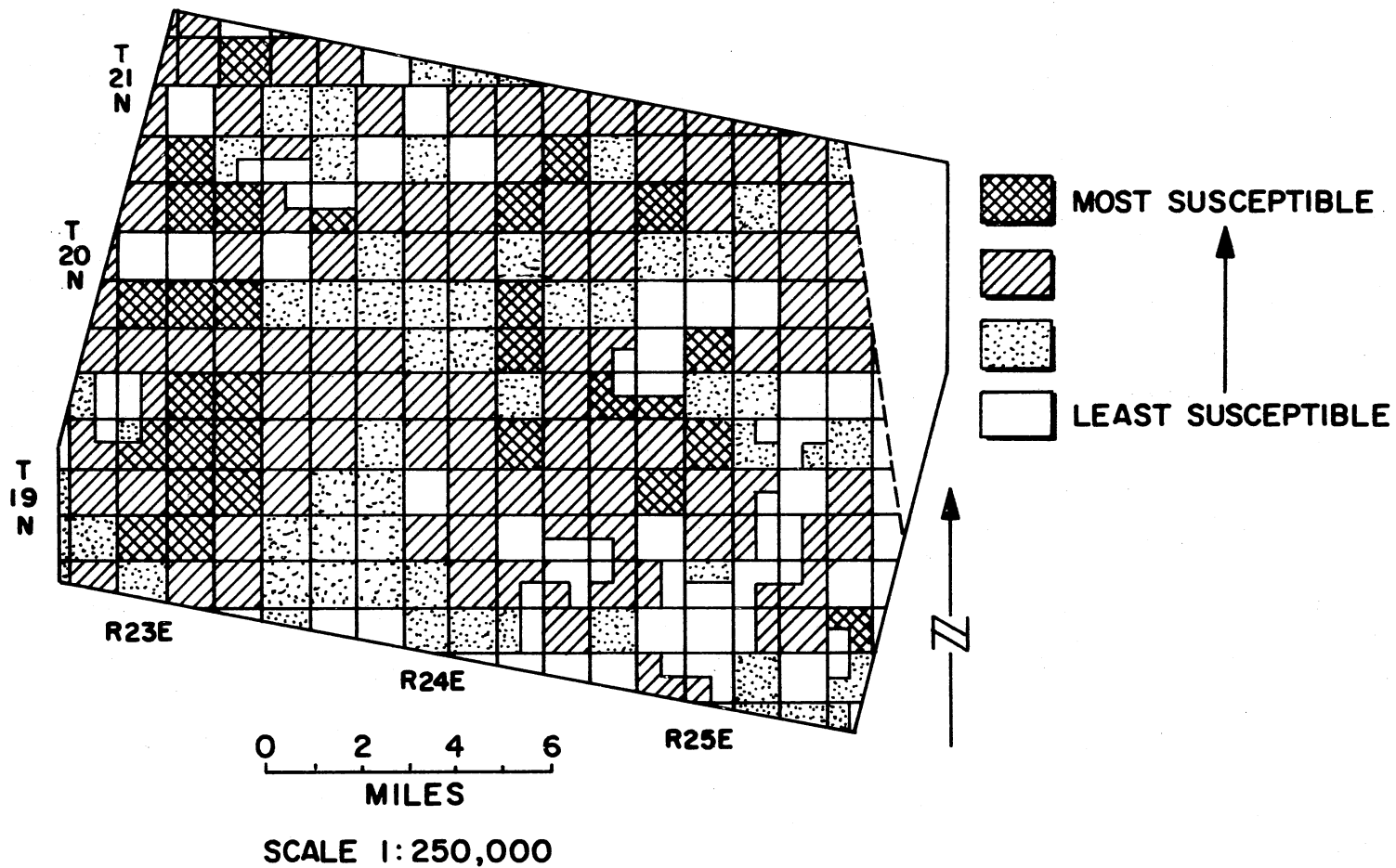


Figure 26 - Pollution Susceptibility Map of the Subscene Study Area Derived From Skylab-4 Photography

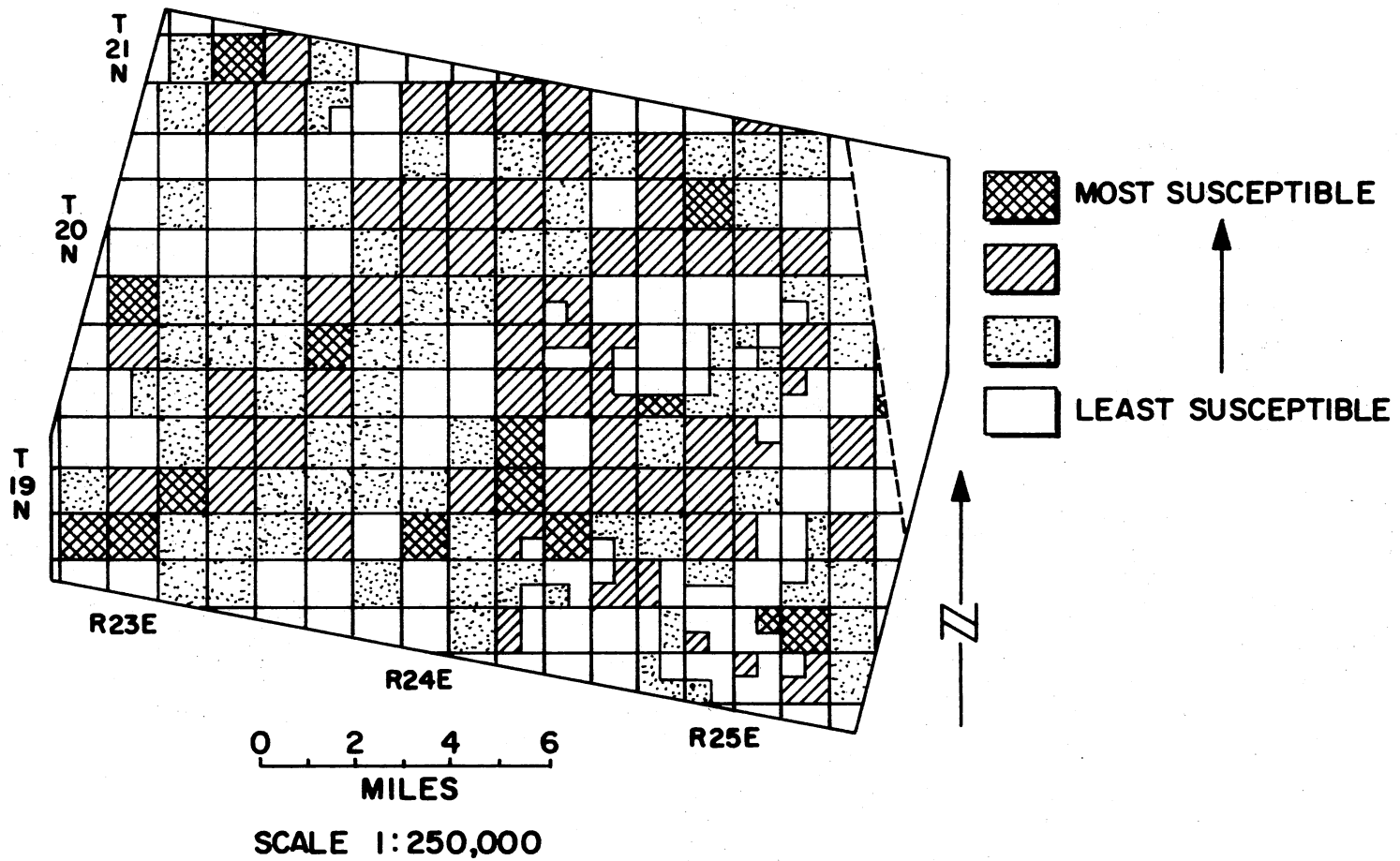


Figure 27 - Pollution Susceptibility Map of the Subscene  
 Study Area Derived From Composite Digital  
 Imagery (PC-1, 2; ratio of 5/7)

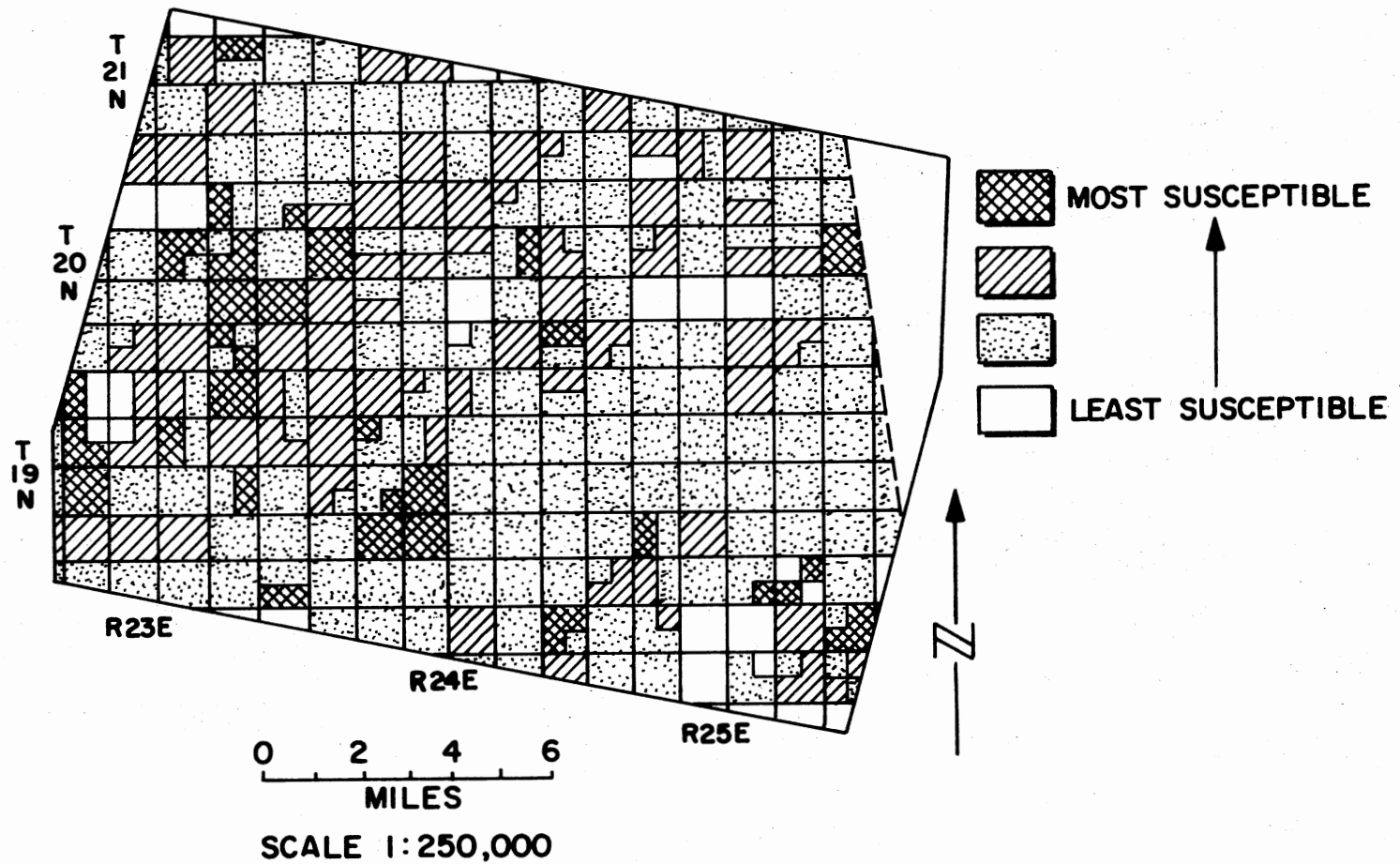


Figure 28 - Pollution Susceptibility Map of the Subscene Study Area Derived From Drainage Data

TABLE VIII  
COMPARISON OF POLLUTION SUSCEPTIBILITY MAPS

Map Source	Pollution Susceptibility Classes	Percentage of Subscene Area			
		1	2	3	4
Standard LANDSAT imagery		10	37.5	29.5	23
Computer-enhanced digital imagery		10.5	32	31.5	26
Skylab-4		13	45	23	19
Composite digital imagery		7	28	32.5	33
Drainage		10	25	57.5	7.5

areas (class 3) is higher when based on drainage data derived from photographic maps.

## Statistical Analyses of Water Quality for Pollution Susceptibility Evaluation

### Method

The variability of ground-water quality and well yield was compared with linear density and predicted level of pollution susceptibility. The map in Figure 29 shows the location of wells and springs from which water quality data are available. This map was superimposed onto the pollution susceptibility maps prepared from linear densities, number of intersections, and drainage density. The wells and springs located in the highest and lowest susceptible areas were classified and placed in three classes--1 & 2, 3, and 4, respectively. Class 1 & 2, for example, includes wells associated with the highest susceptible areas whereas wells located within the least susceptible area are included in class 4. Water quality data were identified with each class; collected and reported data are also differentiated. Analysis of variance was used to compare each chemical constituent with classes 1 & 2, 3 and 4. The data used for the analyses of variance in obtaining the F-distribution is included in Appendix C; the procedure of the statistical analyses of water quality is given in Appendix D. The procedure is also described by Huntsberger (1964). Analyses of water quality for collected and reported data are given in Tables IX and X. The analyses of variance used for each type of pollution susceptibility map is shown for standard LANDSAT imagery in Table XI, for digital imagery (PC-1, 2)

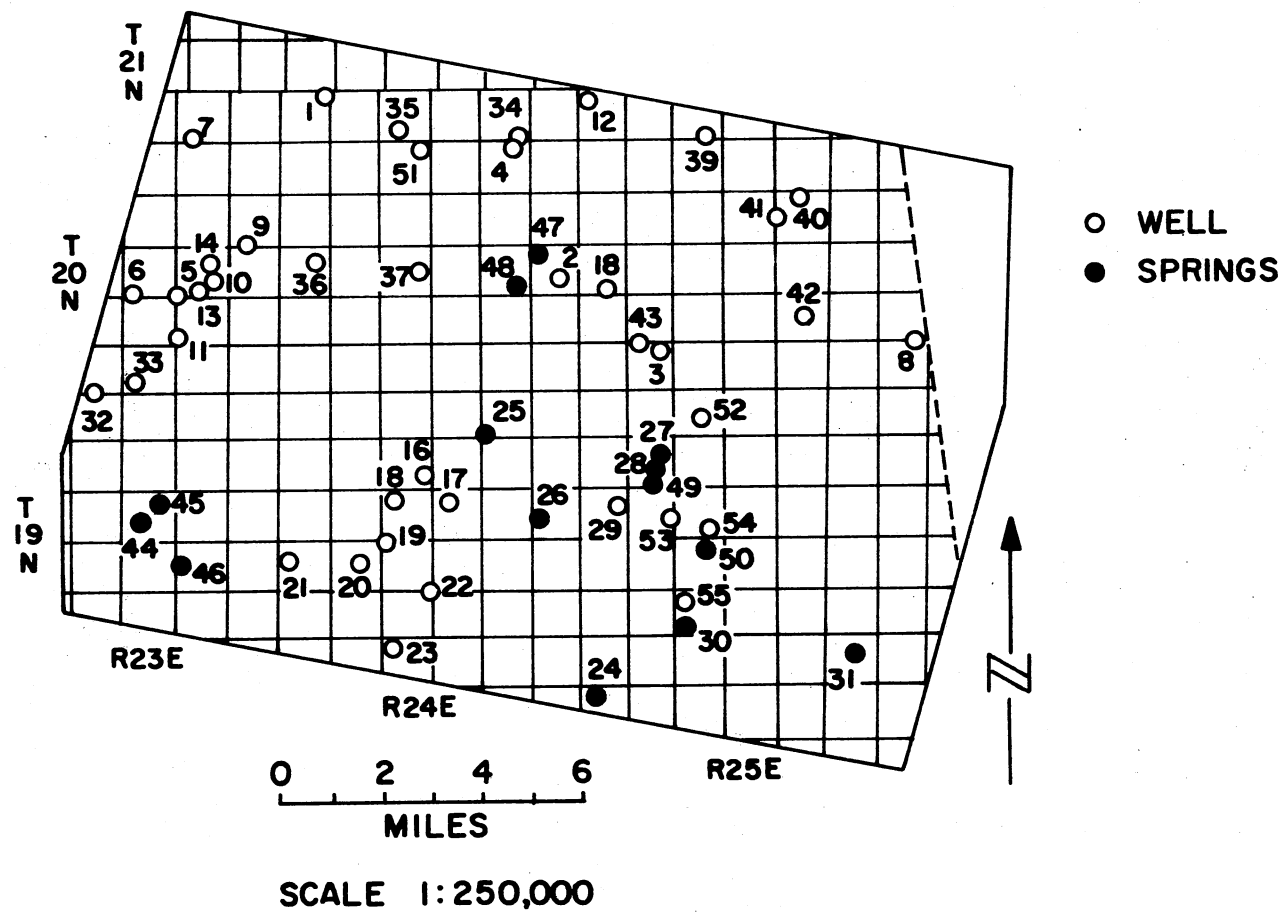


Figure 29 - Location Map of Springs and Wells

TABLE IX  
CHEMICAL ANALYSES OF WATER COLLECTED BY THE AUTHOR FROM WELLS AND SPRINGS\*

Sample	Quality														
	Sodium (%)	SAR	Hardness	Cl	SO <sub>4</sub>	NO <sub>3</sub>	Fe	TDS	pH	Na	Mg	Ca	HCO <sub>3</sub>	K	CO <sub>2</sub>
44	7	.2	140	11.7	0.6	8.8	.06	178	8.0	3.4	1.6	54.6	129.3	.31	37.8
45	5	.1	105	8.9	.3	5.3	.09	127	7.5	3.3	1.5	39.8	98.2	.48	0
46	6	.1	80	6.0	1.0	6.6	.09	112	7.9	2.6	1.0	24.5	79.3	.37	0
47	18	.3	45	8.9	.3	7.0	.06	62	7.0	3.6	.9	16.9	28.7	.07	0
48	8	.1	55	10.3	4.9	<4.4	.02	88	7.3	2.3	1.1	20.1	76.9	.23	0
49	9	.1	50	6.0	.1	4.4	.01	85	7.3	2.0	.6	17.1	59.8	<.1	22.8
50	1	.2	45	13.1	.2	5.3	<.01	77	7.0	2.9	.8	16.5	53.7	.1	0
51	6	.1	85	11.7	.1	9.7	<.01	157	7.5	3.3	.8	32.5	142.7	<.1	7.8
52	15	.3	85	19.2	0.0	67.8	<.01	218	7.5	6.0	2.0	30.9	101.9	<.1	0
53	53	1.9	70	32.7	8.8	4.8	.01	268	7.8	37.3	5.9	17.1	10.8	2.39	37.8
54	59	1.7	35	20.6	5.1	7.0	.02	157	7.8	23.4	1.8	10.4	86.6	.86	0
55	6	.1	145	13.1	.2	12.8	.01	131	7.1	3.0	.9	27.9	94.6	.71	0

\*All values are in parts per million (ppm) except pH, sodium absorption ratio (percent), and conductivity.

TABLE X  
 CHEMICAL ANALYSES OF WATER SAMPLES\*

Sample Number	Well Yield	Hardness	Cl	SO <sub>4</sub>	NO <sub>3</sub>	Fe	TDS	pH
1	***	228	10.0	17.0	<.1	<.1	304.0	7.8
2	3.0	71.0	118	<5.0	<.1	0.1	369	7.9
3	6.0	68.0	11.0	<2.0	714.0	<.1	84.0	6.9
4	3.0	233	2.0	23.0	0.3	.40	186.0	7.3
5	8.0	168	4.0	3.0	0.4	0.3	189.0	7.7
6	1.75	212	38.0	13.0	0.4	<.1	246.0	7.8
7	15	140	7.0	5.0	<.1	<.1	337.0	7.9
8	4.5	216	7.0	<2.0	1.8	0.15	190.0	7.6
9	3.0	200.0	3.0	5.0	0.2	.08	227.0	8.0
10	***	144.0	28.0	18.0	0.4	0.9	211.0	7.4
11	4.0	650	8.0	3.0	0.8	0.08	110.0	6.7
12	3.0	191.0	7.0	10.0	0.6	<0.05	168.0	7.7
13	20.0	145.0	8.0	5.0	1.3	<0.05	160.0	7.3
14	***	116.0	32.0	15.0	.4	0.2	205.0	7.8
15	1.0	70.0	12.0	7.0	2.0	0.10	153	7.7
16	***	122.0	14.0	3.0	<.1	<.1	261.0	***
17	***	175.0	11.0	3.0	<.1	.38	282	***
18	***	103.0	69.0	10.0	<.1	.10	307	***
19	***	233.0	6.0	30.0	1.3	.1	254	***
20	***	315.0	11.0	50.0	<.1	<.1	388	***
21	***	123.0	25.0	36.0	<.1	<.1	263	***
22	***	42	10.0	3.0	<.1	.1	374	***
23	***	119	84.0	19.0	.2	.13	190	***
24	30	151-200	11-25	11-25	***	***	***	***
25	***	151-200	11-25	26-50	***	***	***	***
26	650	151-200	11-25	11-25	***	***	***	***
27	***	101-150	11-25	26-50	***	***	***	***



TABLE X (Continued)

Sample Number	Well Yield	Hardness	Cl	SO <sub>4</sub>	NO <sub>3</sub>	Fe	TDS	pH
28	***	151-200	11-25	26-50	***	***	***	***
29	***	74	4.0	2.5	0.2	***	257	
30	610	58	0.2	1.0	4.9	***	83	
31	***	6-10	11-25	11-25	***	***	***	
32	1	151-200	11-25	26-50	***	.51-1	***	
33	75	101-150	11-25	***	***	***	***	
34	***	101-150	11-25	***	***	***	***	
35	5	151-200	11-25	***	***	***	***	
36	***	28	42.0	26.0	32.0	***	230	
37	***	151-200	11-25	26-30	***	.31-.5	***	
38	***	***	***	51-100	***	***	***	
39	72	26	0.2	.2	3.2	***	106	
40	***	151-200	11-25	51-100	***	***	***	
41	***	>1000	11-25	26-50	***	.31-.50	***	
42	15.0	0-10	26-100	101-150	***	***	***	
43	***	82	4.0	1.5	10.0	***	101.0	

\* All values are in parts per million (ppm) except pH and well yield (gpm), gallons per minute

Source: U. S. Department of Health Service

\*\*\* Data not available

TABLE XI  
 STATISTICAL ANALYSES OF WATER QUALITY FOR POLLUTION SUSCEPTIBILITY  
 CLASSES DERIVED FROM STANDARD LANDSAT IMAGERY

Chemical Constituent	Classes			F	OSL
	1&2	3	4		
Fe	0.095	0.126	0.34	4.91	0.02
SO <sub>4</sub>	16.17	16.33	27.68	1.092	0.33
Cl	17.45	18.66	25.78	0.523	0.60
NO <sub>3</sub>	5.64	1.45	5.6	0.0169	0.975
Hardness	120.95	133.14	154.25	1.038	0.35
TDS	159.66	213.23	186.33	1.353	0.25
Well yield	21.14	11.68	10.39	1.854	0.20

All values are in parts per million (ppm) except well yield (gpm).

Symbols: Fe = iron; SO<sub>4</sub> = sulfate; Cl = chloride; NO<sub>3</sub> = nitrate;  
 TDS = total dissolved solids; F = F-distribution;  
 OSL = observed significance level. (Note: A low sig-  
 nificance level would indicate that there is a signif-  
 icant difference among the means.)

in Table XII, for Skylab-4 photography in Table XIII, and for composite digital imagery in Table XIV.

The analysis of variance for pollution susceptibility maps of number of intersections and drainage density did not show any significant level. This was due to an inadequate number of sample data; the number of samples for some of the groups was one or two, and sometimes zero. The statistical results of these analyses for drainage and Skylab numbers of intersections are shown on Tables XV and XVI.

### Results

Comparison and summary of the F-test and corresponding observed significant levels (OSL = .01-.25) are shown in Table XVII. A low observed significant level (high "F" value) would indicate that there is a significant difference among the concentration means or well yield of the pollution susceptibility classes ( 1 & 2, 3 and 4). A significant difference between mean concentrations of chemical constituents and well yield among the pollution susceptibility classes can be noted for each map source. A low observed significant number (OSL) is associated with iron (Fe) and well yield using all map sources except drainage, and with sulfate ( $SO_4$ ), chloride (Cl), hardness, and TDS (total dissolved solids) using only Skylab and digital composite map sources. The Skylab and digital composite map sources provide the greatest number of chemical constituents having significantly different means among the three pollution susceptibility classes.

The summary of statistical means is shown in Table XVIII. Arrows are used to represent the trend of mean values toward an increase in concentration or well yield. Relatively high concentrations and low

TABLE XII  
 STATISTICAL ANALYSES OF WATER QUALITY FOR POLLUTION SUSCEPTIBILITY  
 CLASSES DERIVED FROM DIGITAL IMAGERY (PC-1 & 2)

Chemical Constituent	Classes			F	OSL
	1&2	3	4		
Fe	0.08	0.123	0.31	4.63	0.02
SO <sub>4</sub>	15.45	15.52	25.89	0.858	0.40
Cl	13.48	20.22	25.31	0.65	0.55
NO <sub>3</sub>	5.95	1.95	5.89	0.024	0.975
Hardness	107.23	12.62	141.4	1.187	0.30
TDS	167.07	200.46	198.55	1.076	0.67
Well yield	21.7	12.0	9.65	1.46	0.75

All values are in parts per million (ppm) except well yield (gpm).

Symbols: Fe = iron; SO<sub>4</sub> = sulfate; Cl = chloride; NO<sub>3</sub> = nitrate; TDS = total dissolved solids; F = F-distribution; OSL = observed significance level. (Note: A low significance level would indicate that there is a significant difference among the means.)

TABLE XIII

STATISTICAL ANALYSES OF WATER QUALITY FOR POLLUTION SUSCEPTIBILITY  
DERIVED FROM SKYLAB PHOTOGRAPHY

Chemical Constituent	Classes			F	OSL
	1&2	3	4		
Fe	0.07	0.157	0.32	4.92	0.02
SO <sub>4</sub>	9.27	23.34	25.2	1.51	0.25
Cl	13.03	20.94	29.9	2.87	0.10
NO <sub>3</sub>	5.00	1.11	5.62	.028	0.977
Hardness	118.21	121.3	139.6	1.398	0.25
TDS	158.47	228.33	188.33	1.19	0.30
Well yield	19.37	13.33	9.65	1.61	0.23

All values are in parts per million (ppm) except well yield (gpm).

Symbols: Fe = iron; SO<sub>4</sub> = sulfate; Cl = chloride; NO<sub>3</sub> = nitrate; TDS = total dissolved solids; F = F-distribution; OSL = observed significance level. (Note: A low significance level would indicate that there is a significant difference among the means.)

TABLE XIV

STATISTICAL ANALYSES OF WATER QUALITY FOR POLLUTION SUSCEPTIBILITY  
CLASSES DERIVED FROM DIGITAL COMPOSITE IMAGERY

Chemical Constituent	Classes			F	OSL
	1&2	3	4		
Fe	0.075	0.12	0.32	5.54	0.01
SO <sub>4</sub>	12.7	16.91	24.23	.972	0.35
Cl	12.65	20.70	23.46	2.54	0.10
NO <sub>3</sub>	6.37	6.31	4.71	0.067	0.92
Hardness	110.33	121.8	141.84	5.25	0.01
TDS	160.64	202.5	193.11	1.369	0.25
Well yield	22.50	11.79	10.35	1.59	0.23

All values are in parts per million (ppm) except well yield (gpm).

Symbols: Fe = iron; SO<sub>4</sub> = sulfate; Cl = chloride; NO<sub>3</sub> = nitrate; TDS = total dissolved solids; F = F-distribution; OSL = observed significance level. (Note: A low significance level would indicate that there is a significant difference among the means.)

TABLE XV

STATISTICAL ANALYSES OF WATER QUALITY FOR POLLUTION SUSCEPTIBILITY  
CLASSES DERIVED FROM DRAINAGE MAP (aerial photograph)

Chemical Constituent	Classes			F	OSL
	1&2	3	4		
Fe	0.17	0.135	0.15	0.14	0.85
	11.46	17.2	67.33	10.07	-
Cl	18.33	18.72	41.0	1.54	0.25
NO <sub>3</sub>	3.04	4.64	1.8	10.97	0.90
Hardness	118.33	121.9	216.0	1.40	0.25
TDS	190.94	205.0	148.0	0.53	0.40
Well yield	17.75	15.53	9.75	0.083	0.91

All values are in parts per million (ppm) except well yield (gpm)

Symbols: Fe = iron; SO<sub>4</sub> = sulfate; Cl = chloride; NO<sub>3</sub> = nitrate; TDS = total dissolved solids; F = F-distribution; OSL = observed significance level. (Note: A low significance level would indicate that there is a significant difference among the means.)

TABLE XVI

STATISTICAL ANALYSES OF WATER QUALITY FOR POLLUTION SUSCEPTIBILITY  
DERIVED FROM SKYLAB PHOTOGRAPHY (number of intersections)

Chemical Constituent	Classes			F	OSL
	1&2	3	4		
Fe	0.112	0.162	0.164	0.029	0.75
SO <sub>4</sub>	17.9	19.52	16.28	0.065	0.93
Cl	22.63	18.74	17.19	0.272	0.75
NO <sub>3</sub>	6.62	4.32	4.95	0.113	0.86
Hardness	117.11	121.6	138.38	0.75	0.45
TDS	192.12	188.14	206.1	0.139	0.86
Well yield	16.21	43.5	6.68	2.34	0.12

All values are in parts per million (ppm) except well yield (gpm).

Symbols: Fe = iron; SO<sub>4</sub> = sulfate; Cl = chloride; NO<sub>3</sub> = nitrate; TDS = total dissolved solids; F = F-distribution; OSL = observed significance level. (Note: A low significance level would indicate that there is a significant difference among the means.)



TABLE XVII

## SUMMARY OF F-TEST SIGNIFICANCE BETWEEN POLLUTION SUSCEPTIBILITY CLASSES

Chemical Constituent	Map Source	Standard LANDSAT (Neg. 7 and Color)		Digital Imagery (PC-1, 2)		Skylab Photography		Digital Composite		Drainage		Skylab No. Intersection	
		F	OSL	F	OSL	F	OSL	F	OSL	F	OSL		
Fe		<u>4.91</u>	<u>0.02</u>	<u>4.51</u>	<u>0.02</u>	<u>4.92</u>	<u>0.02</u>	<u>5.54</u>	<u>0.01</u>	0.14	0.86	0.029	0.75
SO <sub>4</sub>		1.092	0.33	0.858	0.40	<u>1.52</u>	<u>0.25</u>	0.972	0.35	10.07	-	0.065	0.93
Cl		0.523	0.60	0.65	0.55	<u>2.87</u>	<u>0.10</u>	<u>2.54</u>	<u>0.10</u>	<u>1.54</u>	<u>0.25</u>	0.272	0.75
NO <sub>3</sub>		0.0169	0.975	0.024	0.973	0.028	0.97	0.067	0.92	0.097	0.90	0.113	0.86
Hardness		1.038	0.35	<u>1.187</u>	<u>0.30</u>	<u>1.398</u>	<u>0.25</u>	<u>5.25</u>	<u>0.01</u>	<u>1.49</u>	<u>0.25</u>	0.75	0.45
TDS		<u>1.353</u>	<u>0.25</u>	1.076	0.33	<u>1.19</u>	<u>0.30</u>	<u>1.369</u>	<u>0.25</u>	0.53	0.40	0.139	0.86
Well Yield		<u>1.854</u>	<u>0.20</u>	<u>1.46</u>	<u>0.25</u>	<u>1.61</u>	<u>0.23</u>	<u>1.59</u>	<u>0.23</u>	0.83	0.92	<u>2.34</u>	<u>0.12</u>

Composite map is derived from the line prints of the ratio of Bands 5 to 7 and the positive and negative PC-1 transformation of the multispectral data. Solid lines indicate most significant of prediction level. Dashed lines indicate moderately significant of prediction level. (Derived from Tables IX, X, XI, XII, XIII, AND XIV).

Symbols: Fe = iron; SO<sub>4</sub> = sulfate, Cl = chloride; NO<sub>3</sub> = nitrate; TDS = total dissolved solids; F = F-distribution; OSL = observed significant level. (Note: a low significant level would indicate that there is a significant difference among the means.)

TABLE XVIII  
SUMMARY OF STATISTICAL MEANS FOR CHEMICAL CONSTITUENTS\*

Chemical Constituent	Pollution Susceptibility Map Source	Class	Standard LANDSAT (Neg. 7 and Color)	Digital Imagery	Skylab Photography	Digital Composite	Drainage	Skylab Intersections
Fe	1&2		0.01 ↓ **	0.08 ↓	0.07 ↓	0.08 ↓	0.17 ↓	0.11 ↓
	3		0.31 ↓	0.12 ↓	0.16 ↓	0.12 ↓	0.14 ↓	0.16 ↓
	4		0.34 ↓	0.31 ↓	0.32 ↓	0.32 ↓	0.15 ↓	0.16 ↓
SO <sub>4</sub>	1&2		16.17 ↓	15.45 ↓	9.27 ↓	12.70 ↓	11.46 ↓	17.90 ↓
	3		16.33 ↓	15.52 ↓	23.34 ↓	16.91 ↓	17.20 ↓	19.52 ↓
	4		27.68 ↓	25.89 ↓	25.20 ↓	24.23 ↓	67.33 ↓	16.28 ↓
Cl	1&2		17.45 ↓	13.48 ↓	13.03 ↓	12.65 ↓	18.55 ↓	22.63 ↑
	3		18.66 ↓	20.22 ↓	20.94 ↓	20.70 ↓	18.72 ↓	18.74 ↑
	4		25.78 ↓	25.31 ↓	29.90 ↓	23.46 ↓	41.00 ↓	17.19 ↑
NO <sub>3</sub>	1&2		5.64 ↑	5.95 ↑	5.00 ↑	6.37 ↑	3.04 ↓	6.62 ↑
	3		1.45 ↓	1.95 ↓	1.11 ↓	6.31 ↑	4.64 ↓	4.32 ↓
	4		5.60 ↓	5.89 ↓	5.62 ↓	4.71 ↑	1.80 ↓	4.95 ↓
Hardness	1&2		120.95 ↓	107.23 ↓	118.21 ↓	110.33 ↓	118.33 ↓	117.11 ↓
	3		133.14 ↓	126.20 ↓	121.30 ↓	121.80 ↓	121.90 ↓	121.6 ↓
	4		154.25 ↓	141.14 ↓	139.60 ↓	141.84 ↓	216.00 ↓	138.38 ↓
TDS	1&2		159.66 ↓	167.07 ↓	158.47 ↓	160.64 ↓	190.94 ↓	192.12 ↑
	3		213.23 ↓	200.46 ↓	228.33 ↓	202.50 ↓	205.00 ↓	188.14 ↓
	4		186.33 ↓	198.55 ↓	188.33 ↓	193.11 ↓	148.00 ↓	206.10 ↓
Well yield	1&1		21.14 ↑	21.70 ↑	19.37 ↑	22.50 ↑	17.75 ↑	16.21 ↓
	3		11.68 ↓	12.00 ↓	13.33 ↓	11.79 ↓	15.53 ↓	43.50 ↓
	4		10.39 ↓	9.65 ↓	9.65 ↓	10.35 ↓	9.75 ↓	6.68 ↓

\* Derived from Tables IX, X, XI, XII, XIII, and XIV.

\*\* Arrows signify trend of mean values toward an increase in concentration or well yield.

well yield are generally associated with classes represented by low pollution susceptibility (classes 3 and 4). Exceptions to these trends are noted for nitrate ( $\text{NO}_3$ ) and total dissolved solids (TDS). If the observed significance levels (0.25) for Skylab and digital composite map sources in Table XVII are compared to these trends, it can be concluded that the trends are significant among classes for well yield and all chemical constituents except nitrate. However, if a lower OSL of 0.10 (higher probability that a difference among means exists) is applied to classes derived from Skylab and digital data, a significant trend can be noted for only iron (Fe), chloride (Cl), and hardness. If an OSL of 0.20 is used, the trend of higher well yield with higher levels of pollution susceptibility becomes increasingly significant for classes derived from Standard LANDSAT imagery.

## CHAPTER V

### SUMMARY OF RESULTS

#### Linears

The utility of Skylab-4S190A photography in the first phase of this study was used to identify and compare linear features apparent on the Skylab photography with the **previously** mapped faults and other structural features (syncline and anticline) of the regional area. Twenty-one of the **previously** mapped faults were identified on the Skylab photography. Watts (1977) identified thirteen of the **previously** mapped faults which were indicated on Band 7 of the LANDSAT photo-image. Most of these linears correlated with faults mapped in the Boston Mountain plateau of the Ozark region as well as in western Cherokee and southern Adair Counties. There are four linears in the Springfield structural plain corresponding with known faults. Some of the linears appeared to be parallel to the structural trends of the study area.

Linears mapped from Skylab-4, Band 7 and color composites (4, 5, 7) of LANDSAT photo imagery and computer-enhanced images of the detailed subscene area were not compared directly with the **previously** mapped geologic features, but they compared favorably with each other. The linears exhibited on LANDSAT photo-imagery and computer-enhanced LANDSAT imagery were also identified on Skylab-4 S190A photography.

Watts (1977) reported a similar correlation between trends of

LANDSAT linears and of joints and drainage segments. These measured joint orientations were comparable with all linear maps.

The land-use patterns which had been eliminated from the linear maps were distinguishable on the LANDSAT and digital images. The Skylab-4 S190A photography was more useful than other images for discriminating land use segments such as power lines, gas lines, railroads and highways, but the digitally-enhanced LANDSAT images, particularly the first principal component (PC-1), were useful for land use patterns such as vegetation and small lakes.

#### Pollution Susceptibility

Comparison of pollution susceptibility maps with water quality data indicated that the distribution of pollution susceptibilities derived from the digital composite (Watts, 1977) and Skylab-4 S190A linear density maps were the best for predicting pollution susceptibility. The statistical analyses of water quality and well yield were used to show that iron (Fe), chloride (Cl), total dissolved solids (TDS) are significantly different among pollution susceptibility classes. The low observed significance level indicates that there is a significant difference among the means. The directional trend of statistical means for these elements and well yield indicate that high pollution susceptibility can be related to low chemical concentrations and high well yield. A high probability that the trend occurs is indicated by the low observed significance level among the means.

The observed trends are to be expected if it is assumed that ground water is low in concentration due to the effects of dilution within the more densely fractured zones overlain by permeable soils (pollution

susceptibility classes 1 & 2). Therefore, high recharge rates are expected where permeable soils and more densely fractured areas occur. High pollution levels can be expected where point sources of pollution overlie high recharge areas. Because some observed water quality and well yield trends are statistically significant, it can be concluded that Skylab and LANDSAT imagery might be used to produce pollution susceptibility maps for similar fractured limestone and chert aquifers.

#### Recommendations for Future Studies

It is recommended that more water samples be taken (at least two samples for each square mile) so that the statistical analyses of water quality can be studied more precisely (fifty-five samples were used for a 215-square mile area--one sample for every four square miles).

## BIBLIOGRAPHY

- Angusawatana, P. et al., 1974, Earth's Application in Thailand. Presented at Ninth International Symposium on Remote Sensing of the Environment, April 15-19, 1974, Proceedings, Environmental Research Institute of Michigan, pp. 341-361.
- Chavez, Pat S. Jr., Berlin G. Lennis, and Alex V. Acosta, 1976, Linear Enhancement in Southwestern Jordan: U. S. Geological Survey, Flagstaff, Arizona, 86001.
- Clark, E. L., and T. R. Beveridge, 1962, Sixteenth Regional Field Conference Guide Book, Kansas Geological Society.
- Cline, L. M., 1934, Osage Formation of Southern Ozark Region, Missouri, Arkansas and Oklahoma: American Association Petroleum Geologist, Bull. Vol. 18, pp. 1132-1159.
- Ebtehadj, K., 1973, Application of ERTS-1 Imagery in the Field of Geology, Agriculture, Forestry, and Hydrology to Selected Test Sites in Iran: Symposium on Significant Results Obtained From Earth Resource Technology Satellite, Vol. 1, Sec. 13, pp. 1699-1714.
- Edwin, W. Reed, Stuart L. Schoff, and Carl C. Branson, 1955, Ground Water Resources of Ottawa County, Oklahoma: Oklahoma Geological Survey Bull. 72, pp. 128-138.
- El Shazley, A., M. A. Abdel-Hady, M. A. El Ghawaby, and I. A. El Kassas, 1974, Geologic Interpretation of ERTS-1 Images for East Aswan Area, Egypt: In Ninth International Symposium on Remote Sensing of Environment, April 15-19, 1974: Proceedings Environmental Research Institute of Michigan, Ann Arbor, pp. 105-131.
- Garner, G. L., 1965, Aerial Geology of the Flint Area, Delaware County, Oklahoma: Unpublished M. S. Thesis, University of Oklahoma, Norman, Oklahoma, 56 pp.
- Harbaugh, J. W., 1957, Mississippian Bioherms in Northeastern Oklahoma: American Association of Petroleum Geologists Bull. V, 41, pp. 2530-2544.
- Hayes, C. W., 1894, The Overthrust Faults of the Southern Appalachians: Geol. Soc. America Bull. Vol. 2, pp. 141-154.
- Hopkins, T. C., 1893, Marbles and Other Limestones: Arkansas Geological Survey, Annual Report for 1893, Vol. 4, pp. 233-239.

- Huffman, G. G. et al., 1958, Geology of the Flanks of the Ozark Uplift Northeastern Oklahoma: Oklahoma Geological Survey Bull. No. 77, 281 pp.
- Huffman, G. G., and J. N. Starke, 1960, Noel Shale in Northeastern Oklahoma: Oklahoma Geological Survey, Oklahoma Geological Notes, Vol. 20, No. 7, pp. 159-163.
- Huntsberger, V. David, 1964, Elements of Statistical Inference, Iowa State University Press, Ames, Iowa, pp. 213-228.
- Ireland, H. A. 1944, Subsurface Lower Ordovician and Upper Cambrian Formations of Northeastern Oklahoma: U. S. Geological Survey Oil and Gas Investigations, Preliminary Chart 5.
- Laudon, L. R., 1939, Stratigraphy of Osage Subseries of Northeastern Oklahoma: American Association of Petroleum Geologist Bull., Vol. 23, pp. 325-338.
- Marcher, M. V., 1969, Reconnaissance of the Water Resources of the Fort Smith Quadrangle, East Central Oklahoma: Oklahoma Geological Survey Hydrologic Atlas, HA-1, four maps.
- Miser, H. D., and A. H. Purdue, 1916, U. S. Geological Survey: Geological Atlas, Eureka Springs and Harrison Folio No. 202.
- Moore, R. C., 1928, Early Mississippian Formations of the Ozark Region: Missouri Bureau of Geology and Mines, 2nd Series, Vol. 21, 283 pp.
- Ostle, Bernard, 1966, Statistics in Research: Iowa State University, Ames, Iowa, pp. 529-543.
- Owen, D. D., 1852, Report of Geological Survey of Wisconsin, Iowa, and Minnesota and Incidentally of a Portion of Nebraska Territory: Philadelphia, Pennsylvania, pp. 91-92.
- Penrose, R. A. F., 1891, Manganese: Its Uses, Ores and Deposits: Arkansas Geological Survey, Annual Report for 1890, Vol. 1, pp. 113-114.
- Purdue, A. H., G. I. Adams, and E. O. Ulrich, 1904, Zinc and Lead Deposits of Northern Arkansas: U. S. Geological Survey, Prof. Paper PP. Q-24.
- Russell, O. R., F. J. Webber, C. E. Weir, and R. Amato, 1972, Application of ERTS-1 and Aircraft Imagery to Mined Land Investigations: In Remote Sensing of Earth Resources, Vol. 2, pp. 1095-1106.
- Simonds, F. W., 1891, The Geology of Washington County, Arkansas: Arkansas Geol. Survey Annual Report 1888, Vol. 4, pp. 27-37.



- Snider, L. C., 1915, Geology of a Portion of Northeastern Oklahoma: Oklahoma Geolog. Survey Bull. 24, pp. 122.
- Steele, K. F., T. L. Coughlin, H. C. MacDonald, and G. H. Wagner, 1976, Relationship Between Linears and Water Quality in a Carbonate Terrain: G. S. A. Abstract With Programs, 1976, South Central Section, Houston, Texas, pp. 66-67.
- Taff, J. A., 1909, U. S. Geological Survey Atlas: Tahlequah Folio, No. 122.
- Ulrich, E. O., 1911, Revision of the Palezoic System: Geolog. Soc. America Bull. Vol. 22, pp. 281-680.
- United States Department of Agriculture, 1965: Soil Survey Adair County, Oklahoma, pp. 62.
- United States Department of Agriculture, 1970: Soil Survey, Cherokee and Delaware Counties, Oklahoma, pp. 74.
- Wagner, G. H., K. F. Steele, H. C. MacDonald, and T. L. Coughlin, 1976, Water Quality as Related to Linears, Rock Chemistry, and Rain Water Chemistry in a Rural Carbonate Terrain: Journal of Environmental Quality, Vol. 5, No. 4, pp. 441-451.
- Watts, K. R., 1977, Assessment of LANDSAT Imagery for the Investigation of Fracturing: Unpublished M. S. Thesis, Oklahoma State University, Stillwater, Oklahoma, 35 pp.
- White, Luther H., 1926, Subsurface Distribution and Correlation of Pre-Chattanooga "Wilcox" Sand Series of Northeastern Oklahoma: Oklahoma Geological Survey Bull. 40-B.

APPENDIX A

GEOLOGIC FORMATION CHARACTERISTICS

## Cotter Dolomite

Ulrich (1911) named exposures of Cotter, Baxter County, Arkansas, "Cotter dolomite." Although he applied the same term to Jefferson City limestone, it was later concluded that the Jefferson City limestone of that type is older than Cotter. The terms "Turkey Mountain" and "Ordovician silicious limestone" were applied to the Cotter in northeastern Oklahoma by White (1926).

The Cotter is a white-to-gray dolomite with some minor amounts of sandstone, chert, and conglomerate. Exposures of the Cotter are described by Huffman (1958) as occurring near Flint (south of Oklahoma Highway 33) and along the Illinois River Sections 5, 6, 7, and 8, Twp. 19 North, Range 25 East. The Flint outcrop is made up of a lower part of a massive layer of white, slightly sandy, fine-to-medium crystalline dolomite separated by a thin shale bed from upper dolomite. The middle unit consists of massive-to-thin bedded and dense-to-finely crystalline dolomite. The upper portion consists of gray-to-tan chert in beds of massive and gray-to-white finely crystalline dolomite (Garner, 1965).

The thickness of the Cotter dolomite in northeastern Oklahoma ranges from 1 to 270 feet (Ireland, 1944). The thickness in the thesis area exposure is less than 14 feet.

The Cotter is classified as lower Ordovician age, Canadian (Huffman, 1958). The Cotter corresponds with west Spring Creek formation of the Arbuckle in central Oklahoma, and within the Cotter formation of Arkansas (Garner, 1965).

The Cotter dolomite contains weathered granite pebbles and overlies

the Spavinaw granite directly. The Burgen sandstone rests on the Cotter.

#### Burgen Sandstone

The Burgen sandstone was first named by Taff (1905) for the outcrops in Burgen Hollow, northeast of Tahlequah in northern Cherokee County, Oklahoma. The Burgen is a massive white sandstone with thin sandy dolomite. It occurs locally in southern Delaware County approximately one-half mile south of Flint Creek on Oklahoma Highway 33. The Burgen sandstone contains some shale and dolomitic limestone.

#### Chattanooga Shale

The exposure of black shale near Chattanooga, Tennessee, first was named Chattanooga shale by Hayes (1894). At Noel, Missouri, a similar shale was named Noel shale by Adams (1904), and in Arkansas it is called Eureka. The term "Chattanooga Formation" was extended into northeastern Oklahoma by Taff (1909) and by Huffman and Starke (1960). Taff recognized Sylamore Sandstone Member at its base. The Chattanooga Formation consists of hard, fissile, well-jointed black shale, with a local sandstone member, the Sylamore and Noel, at its base. The Chattanooga Formation of Oklahoma has been correlated as upper Devonian-lower Mississippian in age (Huffman and Starke, 1960).

#### Sylamore Sandstone Member

The name "Sylamore" was applied for the exposure of sandstone in the vicinity of Sylamore Creek, Stone County, Arkansas, by Braner (Penrose, 1891). It crops out in northeastern Oklahoma within the

study area along Falls Branch, Black Fox Hollow, along the Illinois River, and along Flint Creek near Flint Oklahoma (Watts, 1977).

The Sylamore varies in thickness (0-18 feet) in Section 23, Twp. 20 North, Range 24 East (Garner, 1967).

The Sylamore Sandstone forms the base of Chattanooga shale. It lies upon the Tyner-Fite-Ferndale sequence (Ordovician) along the upper part of the Illinois River Valley in Oklahoma. The Sylamore Sandstone is believed to be the equivalent of the Misener Sand of the Oklahoma subsurface and Hardin Sandstone of Tennessee. The Sylamore is a white phosphatic Sandstone with a "salt and pepper" appearance on a fresh surface. The sand grains have well-developed crystal faces (Huffman and Starke, 1960).

#### Noel Shale

Huffman and Starke (1960) applied the term "Noel" to the black shale of the upper Chattanooga Formation (shale) in northeastern Oklahoma. As Huffman et al. (1958) reported, this term was used to describe the black shale exposed near Noel, Missouri, by Adams (1904). Noel shale in the study area occupies the valley of the Illinois River and its tributaries, in Flint Creek and at the west end of Lake Frances in Adair County.

The Noel is a black, fissile and pyritic shale which is well-jointed. The joint surfaces are commonly iron-stained. It is of uniform thickness (40 to 60 ft), but a thickness of 88 feet was observed on the water well log of the study area.

## Boone Formation

The term "Boone" was applied by Braner to the rocks of Osagean age in Boone County, Arkansas. It was introduced into geologic literature by Simonds (1891) and Penrose (1891). The term was extended into Oklahoma by Taff (1905).

The Osagean rocks in northeastern Oklahoma were studied by Cline (1934) and Laudon (1939). Laudon divided the Osage series into three formations: the St. Joe Limestone at the base, followed in ascending order by the Reed Springs and Keokuk Formations, which consist of chert and limestone.

### St. Joe Limestone Member

The limestone outcrops of St. Joe, Searcy County, Arkansas, at the basal member of the Boone Formation were named "St. Joe" by Hopkins (1893). Taff (1905) and Cline (1934) identified the St. Joe in northeastern Oklahoma, and Laudon (1939) recognized a "reef phase" and a "non-reef phase." Clark and Beveridge (1952) raised the St. Joe of Missouri to group rank and divided it into three formations which are, in ascending order, Compton, Northview, and Pierson Formations.

The St. Joe is distributed rather widely in northeastern Oklahoma. It crops out along the Illinois River, Flint Creek, and in Calunchety Hollow, Section 13, Twp. 20 North, Range 24 East (Garner, 1965). Three units (Compton, Northview, and Pierson) are recognized within the St. Joe in the thesis area. The lower bed is a gray, medium crystalline limestone, with a thickness of two to ten feet. Watts (1977) reported that it is best developed below Lake Frances dam. The middle

bed of the St. Joe limestone is a green-gray shaley limestone with some calcareous shale and a thickness of from zero to six feet. The upper unit consists of a gray, thick-bedded medium-to-coarsely crystalline limestone. The thickness of the Pierson unit normally varies from three to six feet, but Garner (1965) reported a thickness of 70 feet in Section 13, Twp. 20 North, Range 24 East, where bioherms are developed (Watts, 1977).

#### Reed Springs Chert Member

Moore (1928) applied the term "Reed Springs" Member of the Boone Formation to the exposure of limestone and cherts of Osagean age near Reed Springs in southwestern Missouri. The Reed Springs is exposed in much of northeastern Oklahoma, along the Illinois River in the thesis area. The contact of St. Joe and Reed Springs limestone was observed in Section 35, Twp. 20 North, Range 24 East.

The Reed Springs Chert Member of the Boone Formation consists of thin, alternating beds of gray limestone and dark gray to blue-gray chert. The individual beds of chert and limestone are locally irregular bedded. Small scale fractures and major joints on Reed Springs Formation were reported by Watts (1977). A maximum thickness of 175 feet was reported by Huffman (1958), and an average thickness of 100 feet in the subscone study area was reported by Garner (1965) and Watts (1977). The contact of the Reed Springs and the Keokuk is not well exposed because of the rubble cover from the highly fractured Keokuk Formation.

### Keokuk Chert Member

The limestone exposed near Keokuk, Iowa, was named "Keokuk" by Owen (1852). The term Keokuk was extended to southwestern Missouri by Moore (1933). Snider (1914) recognized fossils of Keokuk age in the Boone Formation of northeastern Oklahoma, and Laudon (1939) applied the term Keokuk to the Osagean chert and limestone overlying the Reed Springs Formation.

The Keokuk Chert exposure forms much of the surface rock in the Springfield structural plain in the thesis area; it crops out in northern Adair and Cherokee Counties. The Keokuk Chert is essentially a massive, white-to-buff fossiliferous chert and is highly fractured. It is interbedded with irregular stringers and masses of blue-gray and fine-grained limestone (Huffman et al., 1958). The chert of the Keokuk is locally tripolitic and weathers red-brown; well drillers refer to it as "cotton rock" (Watts, 1977). Huffman et al. (1958) reported ten feet of white oolitic limestone at the top of the Keokuk; it is like the Short Creek oolite of Ottawa County and southwestern Missouri. Large crinodial reefs or bioherms have been reported in the Keokuk of northeastern Oklahoma by Harbaugh (1957). The thickness of Keokuk ranges from <1 to 250 feet (Huffman et al., 1958).

### Moorefield Formation

The term "Moorefield" was applied to beds between the Boone Chert and the Batesville Sandstone as developed near Moorefield, Arkansas, by Purdue, Ulrich, and Adams (1904). Huffman (1958) subdivided the Moorefield Formation of northeastern Oklahoma into four members: a lower



glaucconitic limestone (the Tahlequah Member; an argillaceous Bayou Manard Member; a chert-pebble calcarenite facies; the Lindsey Bridge Member); and the Ordinance Plant Siltstone and Shale Member. The Moorefield in the thesis area crops out in Section 4 and Section 13, Twp. 20 North, Range 23 East; it is an irregular-bedded argillaceous limestone (Garner, 1967). Its thickness varies from <1 to 18 feet.

#### Hindsville Formation

The term "Hindsville" was used for the limestone exposures near Hindsville, Arkansas, by Purdue and Miser (1916). Huffman et al. (1958) applied the term Hindsville to the rock between Moorefield and Fayetteville Formations in northeastern Oklahoma. The Hindsville consists of gray, medium-grained crystalline, fossiliferous limestone; it rests unconformably upon the Keokuk in Section 3, Twp. 20 North, Range 23 East (Garner, 1965). The Hindsville varies from zero to 50 feet in thickness; a maximum thickness of seven feet was reported in the thesis area by Huffman et al. (1958).

APPENDIX B

WATER QUALITY SAMPLE LOCATIONS

TABLE XIX  
WATER QUALITY SAMPLE LOCATIONS

Number	Section	Twp. (North)	Range (East)	County
1	6	20	24	Delaware
2	24	20	24	"
3	32	20	25	"
4	11	20	24	"
5	23	20	23	"
6	22	20	23	"
7	2	20	23	"
8	31	20	26	"
9	24	20	23	"
10	23	20	23	"
11	26	20	23	"
12	6	20	25	"
13	26	20	23	"
14	23	20	23	"
15	19	20	25	"
16	9	19	24	Adair
17	15	19	24	"
18	16	19	24	"
19	19	19	24	"
20	20	19	24	"
21	21	19	24	"
22	28	19	24	"
23	33	19	24	"
24	6	18	25	"
25	2	19	24	"
26	13	19	24	"
27	38	19	25	"
28	8	19	25	"
29	18	19	25	"

TABLE XIX (Continued)

Number	Section	Twp. (North)	Range (East)	County
30	28	19	25	Adair
31	36	19	25	"
32	33	2-	23	Delaware
33	34	20	23	"
34	2	2-	24	"
35	4	20	24	"
36	19	20	24	"
37	21	20	24	"
39	26	20	24	"
39	4	20	25	"
40	14	20	25	"
41	15	20	25	"
42	26	20	25	"
43	32	20	25	"
44	15	19	23	Cherokee
45	15	19	23	"
46	23	19	23	"
47	24	20	24	Adair
48	23	20	24	"
49	17	19	25	"
50	21	19	25	"
51	9	20	24	Delaware
52	4	19	25	Adair
53	17	19	25	"
54	16	19	25	"
55	28	19	25	"

APPENDIX C

VARIANCE TABLES FOR F-DISTRIBUTION

TABLE XX

ANALYSES OF VARIANCE TABLE FOR CHEMICAL CONSTITUENTS RELATED TO POLLUTION SUSCEPTIBILITY CLASSES DERIVED FROM STANDARD LANDSAT IMAGERY\*

		df	SS	MS	F	OSL
Fe	Among group	2	0.31837753	0.1591	4.91	0.02
	Within group	35	1.1335871	0.032		
Cl	Among group	2	474.841	237.4205	0.523	0.33
	Within group	51	23164.42	454.20		
SO <sub>4</sub>	Among group	2	1232.891	616.445	1.91	0.60
	Within group	51	23164.42	454.20		
NO <sub>3</sub>	Among group	2	8.60	4.30	0.0293	0.975
	Within group	36	5278	146.64		
Hardness	Among group	2	6608.15	3304.07	1.12	0.35
	Within group	44	130493.13	2965.75		
TDS	Among group	2	21746	10873	1.353	0.25
	Within group	34	273212.6	8035.66		
Well Yield	Among group	2	754.47	377.23	1.854	0.20
	Within group	22	4477	203.50		

Symbols: df = degree of freedom; SS = sum of squares; MS = mean square; F = F-distribution; OSL = observed significance level. (Note: A low significance level would indicate that there is a significant difference among the means.)

\*Neg. 7 and Color.

TABLE XXI

ANALYSES OF VARIANCE TABLE FOR CHEMICAL CONSTITUENTS RELATED TO POLLUTION SUSCEPTIBILITY CLASSES DERIVED FROM DIGITAL IMAGERY (PC-1, 2)

		df	SS	MS	F	OSL
Fe	Among group	2	0.301673	0.1508	4.63	0.02
	Within group	35	1.138327	0.0325		
Cl	Among group	2	517.354	256.67	0.67	0.40
	Within group	51	17642.574	385.148		
SO <sub>4</sub>	Among group	2	615.228	307.6	0.858	0.55
	Within group	49	22144.18	461.33		
NO <sub>3</sub>	Among group	2	6.12	3.06	0.024	0.975
	Within group		4610	128.05		
Hard- ness	Among group	2	7806.97	3903.48	1.187	0.30
	Within group	44	144668.03	3288.36		
TDS	Among group	2	8732	4366.3	1.046	0.33
	Within group	34	142049.0	4177.93		
Well Yield	Among group	2	607.49	303.74	1.46	0.25
	Within group	22	4572	207.85		

Symbols: df = degree of freedom; SS = sum of squares; MS = mean square; F = F-distribution; OSL = observed significance level. (Note: A low significance level would indicate that there is a significant difference among the means.)

TABLE XXII

ANALYSES OF VARIANCE TABLE FOR CHEMICAL CONSTITUENTS RELATED TO POLLUTION SUSCEPTIBILITY CLASSES DERIVED FROM SKYLAB PHOTOGRAPHY

		df	SS	MS	F	OSL
Fe	Among group	2	0.3196	0.1598	4.92	0.02
	Within group	35	1.1332	0.03237		
Cl	Among group	2	2373.644	1186.822	2.87	0.25
	Within group	51	21094.282	413.613		
SO <sub>4</sub>	Among group	2	1823	911.5	1.51	0.10
	Within group	49	29319.003	600.8125		
NO <sub>3</sub>	Among group	2	11.67	5.83	.028	0.97
	Within group	36	7697.63	208.044		
Hardness	Among group	2	9530.82	4765.41	1.308	0.25
	Within group	44	149904.18	3406		
TDS	Among group	2	34340.1	17170.05	1.19	0.30
	Within group	34	492044.2	14471.882		
Well Yield	Among group	2	704.74	352.37	1.61	0.23
	Within group	22	4796	218		

Symbols: Df = degree of freedom; SS = sum of squares; MS = mean square; F = F-distribution; OSL = observed significance level. (Note: a low significance level would indicate that there is a significant difference among the means.)



TABLE XXIII

ANALYSES OF VARIANCE TABLE FOR CHEMICAL CONSTITUENTS RELATED TO POLLUTION SUSCEPTIBILITY CLASSES DERIVED FROM COMPOSITE DIGITAL IMAGERY\*

		df	SS	MS	F	OSL
Fe	Among group	2	.3467084	.1733542	5.54	0.01
	Within group	35	1.0950232	.0312863		
Cl	Among group	2	2134.148	1097.074	2.54	0.35
	Within group	51	22000.946	431.946		
SO <sub>4</sub>	Among group	2	1099.243	549.6215	.942	0.10
	Within group	49	27695.547	565.21		
NO <sub>3</sub>	Among group	2	19.7762	9.8881	.0669	0.92
	Within Group	36	3515.0652	147.6407		
Hard- ness	Among group	2	33037.55	16518.77	5.25	0.01
	Within group	44	138276.4	3142.64		
TDS	Among group	2	13171.7	6385.85	1.368	0.25
	Within group	34	171091.8	5032.11		
Well Yield	Among group	2	674.82	337.41	1.57	0.23
	Within group	22	4654	211		

Symbols: Df= degree of freedom; SS = sum of squares; MS = mean square; F = F-distribution; OSL = observed significance level. (Note: a low significance level would indicate that there is a significant difference among the means.)

\* (PC-1,2; Ratio of 5/7).

APPENDIX D

PROCEDURE OF ANALYSES OF WATER QUALITY

DATA FOR F-TEST DISTRIBUTIONS

## Procedure

1. Calculate the total sum of squares by using the following equation:

$$\text{Total SS} = \sum_i \sum_j Y_{ij}^2 - \frac{Y^2}{N}$$

$Y^2$  = the square of the total sum

$N$  = total number of observed values

$\sum V_{ij}$  = sum of squares

2. Calculate the among groups sum of squares by using the following equation:

$$\sum \frac{Y_i^2}{n_i} - \frac{Y^2}{N}$$

$Y_i^2$  = square of the sum (for each group)

$n_i$  = number of samples (for each group)

3. The within group sum of squares can be calculated by subtracting total sum of squares from the group sum of squares.

4. The degrees of freedom for among group is equal to  $(K-1)$  when  $K$  represents the number of groups.

5. The "within group" degrees of freedom can be calculated from  $(N-K)$ .

6. Mean squares can be calculated by dividing each sum of squares by degrees of freedom.

$$7. F = \frac{\text{among group mean square}}{\text{within group mean square}}$$

8. By having the value for "F" and degrees of freedoms, the probability can be read from the "F" distribution tables (Ostler, 1966).

Example

Fe	Group		
	1&2	3	4
	.1	.1	.3
	.4	.4	.1
	.15	.1	.9
	.1	.08	.2
	.1	.08	.38
	.4	.05	.13
	.01	.05	.75
	.02	.10	.01
	.01	.10	.01
	.01	.1	
	.01	.1	
	.02	.1	
	.01	.41	
		.06	
		.09	
		.06	
Sum	1.04	+ 1.98	+ 2.78 = 5.8
Mean	.08	.123	.31     .152 (sum ÷ n)
$n_1=13$		$n_2=16$	$n_3=9$

Total sum of squares 1

$$\sum_i \sum_j y_{ij}^2 - \frac{y^2}{N} = 2.3289998 - \frac{(5.8)^2}{38} = 1.44$$

The among groups sum of squares (SS) is

$$\sum_i \frac{y_i^2}{N} - \frac{y^2}{N} = \frac{(1.04)^2}{13} + \frac{(1.98)^2}{16} + \frac{(2.78)^2}{9} - \frac{(5.8)^2}{38} = .301673$$

The "within groups" sum of squares (SS) is

$$1.44 - .301673 = 1.138327$$

Source	df	SS	MS	F	OSL
Among groups	2 (3-1)	.301673	.1508 (SS÷2)	4.63	0.02
Within groups	35 (38-3)	1.138327	.0325 (SS÷35)		

$$F = \frac{.1508}{.0325} = 4.63$$

Using the "F" distribution table, the observed significance level for  $F_{4.63}$  with degree of freedom 2 & 35 is equal to 0.02. A low significance level would indicate that there is a significant difference among the means.

2  
VITA

Esmaeil Azimi

Candidate for the Degree of  
Master of Science

Thesis: USE OF REMOTE SENSING FOR FRACTURE DISCRIMINATION AND ASSESSMENT OF POLLUTION SUSCEPTIBILITY OF A LIMESTONE-CHERT AQUIFER IN NORTHEASTERN OKLAHOMA

Major Field: Geology

Biographical:

Personal Data: Born in Ajabshir, Iran, June 23, 1949, the son of Mr. and Mrs. Azimi.

Education: Graduated from Ferdossi High School, Tabriz, Iran, in June, 1968; received the Bachelor of Science degree in Geology from Azarabadegan University, Tabriz, Iran, in June, 1975; completed requirements for the Master of Science degree in Geology from the Oklahoma State University, Stillwater, Oklahoma, in December, 1978.

Professional Experience: Geologist for Iranian National Copper Company, 1975-76; trainee hydrologist for Azarbayejan Underground Water Project in Iran, December, 1974-April, 1975.